9-year trends of PM$_{10}$ sources and oxidative potential in a rural background site in France

Lucille Joanna Borlaza[1*], Samuël Weber[1], Anouk Marsal[1], Gaëlle Uzu[1], Véronique Jacob[1], Jean-Luc Besombes[2], Mélodie Chatain[3], Sébastien Conil[4], and Jean-Luc Jaffrezo[1*]

5   [1]University Grenoble Alpes, CNRS, IRD, INP-G, IGE (UMR 5001), 38000 Grenoble, France

[2]Université Savoie Mont-Blanc, CNRS, EDYTEM (UMR5204), 73000 Chambéry, France

[3]Atmo Grand Est, 67300 Schiltigheim, France

[4]ANDRA, DRD/GES Observatoire Pérenne de l'Environnement, 55290 Bure, France

10   *Correspondence to*: Lucille Joanna Borlaza (lucille-joanna.borlaza@univ-grenoble-alpes.fr) and Jean-Luc Jaffrezo (jaffrezo@univ-grenoble-alpes.fr)

Abstract. Long-term monitoring at sites with relatively low particulate pollution could provide an opportunity to identify changes in pollutant concentration and potential effects of current air quality policies. In this study, a 9-year sampling of PM$_{10}$

15   (particles with an aerodynamic diameter below 10 μm) was performed in a rural background site in France from February 28, 2012 to December 22, 2020. The Positive Matrix Factorization (PMF) method was used to apportion sources of PM$_{10}$ based on quantified chemical constituents and specific chemical tracers from collected filters. Oxidative potential (OP), an emerging health-metric that measures PM capability to potentially cause anti-oxidant imbalance in the lung, was also measured using two acellular assays: dithiothreitol (DTT) and ascorbic acid (AA). The contribution of PMF-resolved sources to OP were also

20   estimated using multiple linear regression (MLR) analysis. In terms of mass contribution, the dominant sources are secondary aerosols (nitrate- and sulphate-rich), associated with long-range transport (LRT). However, in terms of OP contributions, the main drivers are traffic, mineral dust, and biomass burning factors. There is also some OP contribution apportioned to the sulphate- and nitrate-rich sources influenced by processes and aging during LRT that could have encouraged mixing with other anthropogenic sources. The study indicates much lower OP values than in urban areas. A substantial decrease (58% reduction

25   from year 2012 to 2020) in the mass contributions from the traffic factor was found, however, this is not clearly reflected in its OP contribution. Nevertheless, the findings in this long-term study in the OPE site could signal effectiveness of implemented emission control policies, as also seen in other long-term studies conducted in Europe, mainly for urban areas.

1 Introduction

Particulate matter (PM) is a key factor in various environmental concerns affecting public health and climate. An

30   overwhelming part of the scientific literature on chemical characterisation and sources of PM is concerned with urban and populated areas, as they are the places where most emissions originate from and where populations are impacted. Further work

has also been done in more specific areas to try to understand particular processes of aerosol formation and specific sources such as in the boreal forest (Yan et al., 2016), polar environments (Barrie and Hoff, 1985; Moroni et al., 2016), high altitude (Rinaldi et al., 2015), or marine sites (Scerri et al., 2016). Rural sites are of great interest as well because they could represent

35 the regional geochemical background of the atmosphere and potential influence from long-range transport (LRT) of sources. Studies at such sites enable the understanding of large-scale processes (Anenberg et al., 2010; Mues et al., 2013; Konovalov et al., 2009), which is necessary to elaborate chemical transport models. The observation over a long period of time of the geochemical background of the atmosphere can lead to the identification of long-term trends and the effect of recent changes in the source emissions. Indeed, several programmes have been set to monitor atmospheric composition in a harmonised way

40 for background areas throughout Europe and North America. Among these are ACTRIS (Aerosol, Clouds and Trace Gases Research Infrastructure) (Pappalardo, 2018), EMEP (European Monitoring and Evaluation Programme) (Aas et al., 2012; Alastuey et al., 2016), IMPROVE (Interagency Monitoring of Protected Visual Environments) (Hand et al., 2012), and CAPMoN (Canadian Air and Precipitation Monitoring Network) (Nejedlý et al., 1998). However, few sites propose in-depths chemical characterization of PM for periods of about 10 years.

45 Further, although current air quality standards are based on ambient mass concentration of PM, there is also a growing interest in new types of characterization that would take into account not only particle composition but also its capability to generate health impacts (Park et al., 2018; Crobeddu et al., 2017; Møller et al., 2010; Bates et al., 2019). This is the case of the oxidative potential (OP) of PM (Nel, 2005; Conte et al., 2017; Yang et al., 2014; Verma et al., 2014), the ability of PM to generate reactive oxygen species (ROS) leading to PM-induced oxidative stress in the lungs. In France, several studies have reported

50 about OP of ambient PM in different urban environments (Weber et al., 2018, 2021; Borlaza et al., 2021; Calas et al., 2019; Daellenbach et al., 2020), but there are still limited studies performed in rural areas. The characterization of PM sources and OP in a rural site will enable us to see the large-scale effects of mitigation policies that target reduction of PM mass concentrations. This will also provide knowledge of efficiency of current air quality guidelines in terms of other emerging health-based metrics of PM exposure.

55 This study presents the results of a 9-year period of measurement of chemical and OP characteristics of PM_{10} (particles with diameter ≤ 10 µm) in a rural site (hereafter referred to as "OPE") in Houdelaincourt, north-eastern France. The large filter dataset ($n = 434$) led to an extensive source apportionment using Positive Matrix Factorisation (PMF) model. The main drivers of OP of PM_{10} were apportioned to PMF-resolved sources using a multiple linear regression (MLR) model. Finally, this study investigated long-term trends of emission sources and OP to provide insights in the effectiveness of existing air quality policies

60 both in terms of mass concentration and potential exposure to PM.

2 Methodology

2.1 Site description and sampling parameters

The OPE (Observatoire Pérenne de l'Environnement) sampling site is managed by the French national radioactive waste management agency (ANDRA). It is located in a remote area in the north-eastern part of France (48.5°N, 5.5°E) at an altitude
65 of 390 m above sea level, in a large agricultural area without any residential areas within several kilometres (Figure 1). This site, being far from any local anthropogenic sources, is a good representative of the rural atmospheric background of north-eastern France. Golly et al. (2019) also demonstrated that the PM chemistry is very close to that in several other background rural sites in France.

The PM_{10} samples in this study were collected from February 28, 2012 to December 22, 2020. Particularly, from February 28,
70 2012 to December 28, 2015, the samples ($n = 181$) were collected on a weekly basis (from Tuesday 9:00 AM to Tuesday 9:00 AM) using a low volume sampler (Partisol, $1 \, m^3 \, h^{-1}$) onto 47 mm-diameter quartz fibre filters (Tissuquartz PALL QAT-UP 2500 diameter 47 mm). From January 12, 2016 to December 22, 2020, the samples ($n = 253$) were collected on a daily (24-hour) basis in a 6-day sampling interval using a high-volume sampler (Digitel DA80, $30 \, m^3 \, h^{-1}$) onto 150 mm-diameter quartz fibre filters (Tissuquartz PALL QAT-UP 2500 diameter 150 mm).

75 All filters were preheated at 500 °C for 12 hours before use to avoid organic contamination. Blank filters (about 10% by number of the actual filters) were also collected to quantify detection limits and to secure the absence of contamination during sample transport, setup, and recovery. After collection, all filter samples were wrapped in aluminium foil, sealed in zipper plastic bags, and stored at <4 °C until further chemical analysis.
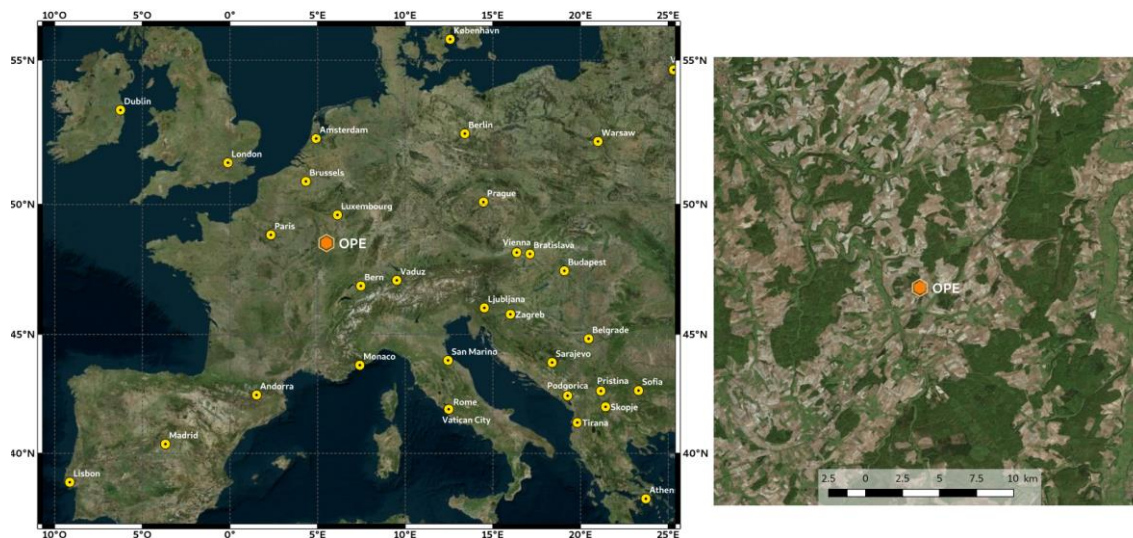
80 **Figure 1: Location of the OPE site in France. ©OpenStreetMap contributors 2020. Distributed under the Open Data Commons Open Database License (ODbL) v1.0.**

2.2 Chemical analyses

After collection, samples were subjected to various chemical analyses to perform the quantification of the major constituents by mass and specific chemical tracers of sources needed for the PMF model. These analyses were performed in the same laboratory for all samples (n=434) during the entire sampling duration (February 28, 2012 to December 22, 2020).

The carbonaceous components (organic carbon (OC) and elemental carbon (EC)) were analysed using a thermo-optical method on a Sunset Lab analyser (Birch and Cary, 1996), using the EUSAAR2 temperature program. Total organic matter (OM) in daily ambient PM_{10} were estimated by multiplying the OC mass concentration by a factor 1.8. Yazdani et al. (2021) showed that this is consistent with the range of ratio estimated for rural samples from the IMPROVE network, that are generally higher than for urban samples.

A set of other chemical analyses was performed on a single water extraction of each filter. This extraction was performed in a 10 ml of ultra-pure water under vortex agitation for 20 minutes. The extract was then filtered with a 0.22 µm porosity Nucleopore filter. The major ionic components (Na^+, NH_4^+, K^+, Mg^{2+}, Ca^{2+}, Cl^-, NO_3^-, SO_4^{2-}) and MSA were measured by ion chromatography (IC, Thermo Fisher ICS 3000) following a standard protocol described in Jaffrezo, et al. (1998) and Waked, et al. (2014). An ICS300 (Thermo-Fisher) with AS11 HC column for the anions and CS16 for the cations was used.

The analyses of anhydro-sugars and primary saccharides were achieved using a high-performance liquid chromatography with pulsed amperometric detection (HPLC-PAD). The samples collected before year 2017 was analysed using a set of Metrohm columns (MetroSep A Supp 15 and Metrosep Carb1) on Dionex DX500 HPLC. The samples collected after year 2017 were analysed with a Thermo-Fisher ICS 5000+ HPLC equipped with 4 mm diameter Metrosep Carb 2×150 mm column and 50 mm pre-column. The analytical run is isocratic with 15% of an eluent of sodium hydroxide (200 mM) and sodium acetate (4 mM) and 85% water, at 1 ml min^{-1}. These methods allowed the quantification of anhydrous saccharides (levoglucosan and mannosan) and polyols (sum of arabitol and mannitol) as described in detail in Waked et al. (2014) and Samaké et al. (2019).

Trace elements were analysed after mineralization, using 5 ml of HNO_3 (70 %) and 1.25 ml of H_2O_2 during 30 minutes at 180 °C in a microwave oven (microwave MARS 6, CEM). The elemental analysis (Al, As, Ba, Ca, Cd, Ce, Co, Cr, Cs, Cu, Fe, K, La, Li, Mg, Mn, Mo, Ni, Pb, Pd, Pt, Rb, Sb, Se, Sn, Sr, Ti, Tl, V, Zn, Zr) was performed on this extract using inductively coupled plasma mass spectroscopy (ICP-MS) (ELAN 6100 DRC II PerkinElmer or NEXION PerkinElmer) as described by Alleman et al. (2010).

All procedures have been performed following the related EN standards (i.e., EN 12341, EN 14902, EN 16909, EN 16913). A quality control of the chemical analyses includes a mass closure test, available in the supplementary information (SI, see S1). Finally, our group successfully and regularly participates in inter-laboratory comparison exercises for OC and EC within ACTRIS, and in EMEP (European Monitoring and Evaluation Programme) for ions analysis.

2.3 Oxidative potential (OP) analysis

The OP analysis was performed on PM_{10} extracts from collected filter samples using a simulated lung fluid (SLF) solution composed of a Gamble + DPPC (dipalmitoylphosphatidylcholine) at 25 µg ml^{-1} iso-mass concentration (Calas et al., 2017). This methodology facilitates particle extraction in conditions closer to lung physiology. The OP analysis started on samples collected from June 13, 2017 to December 22, 2020, amounting to a total of 191 samples.

Two assays were used to characterize OP activity: (1) dithiothreitol (DTT) and (2) ascorbic acid (AA) assays, as briefly described in the following sections. The volume-normalized OP activity (OP_v) is the OP consumption (nmol min^{-1}) normalized by the sampled air volume (m^3), representing the OP exposure in each sample. All samples analysed were subjected to triplicate analysis and each sample results in the mean of such triplicate. The common coefficient of variation (CV) is between 0 and 10% for each assay.

DTT is used as a chemical surrogate to mimic *in vivo* interaction of PM with biological reducing agents in the DTT assay. The consumption of DTT in the assay represents the ability of PM to generate ROS (Cho et al., 2005). The PM_{10} extract is mixed with the DTT solution. Afterwards, the remaining DTT that did not react with PM_{10} is reacted with 5,50-dithiobis-(2-nitrobenzoic acid) (DTNB). This reaction produces 5-mercapto-2-nitrobenzoic acid or TNB. The TNB is measured by absorbance at 412 nm wavelength using a plate-reader (TECAN spectrophotometer Infinite M200 Pro) with 96-well plates (CELLSTAR, Greiner-Bio) in a 10-minute time step interval for a total of 30 minutes of analysis time.

AA is a known antioxidant used in AA assays using a respiratory tract lining fluid (RTFL) (Kelly and Mudway, 2003). This antioxidant prevents the oxidation of lipids and proteins in the lung lining fluid (Valko et al., 2005). The consumption of AA also represents the ability of PM to generate ROS. The mixture (PM_{10} extracts reacted with AA) is injected into a 96-well multiwall plate UV-transparent (CELLSTAR, Greiner-Bio) and measured at 265 nm absorbance using a plate-reader (TECAN spectrophotometer Infinite M200 Pro) in a 4-minute time step interval for a total of 30 minutes of analysis time.

In every experiment, a positive control test is performed to ensure the accuracy and precision of measurements. A 1,4-naphthoquinone (1,4-NQ) solution was used for both DTT (40 µl of 24.7 µM stock solution) and AA (80 µl of 24.7 µM 1,4-NQ solution) assays. The CV of the positive controls were <3% for the 2 assays. Additionally, an ambient filter collected from the lab roof (with an expected constant OP value) was added on each microplate to ensure precision of OP measurements.

2.4 Source Apportionment

2.4.1 PMF model and input variables

The United States Environmental Protection Agency (US-EPA) Positive Matrix Factorization (PMF 5.0) software (Norris et al., 2014) was used to identify and quantify the major sources of PM_{10}. PMF is based on a factor analysis technique fully described by Paatero and Tapper (1994) and is now widely used for source apportionment around the world. Additional information about the model description is provided in the SI (S2).

In this study, 23 chemical species were used as input variables, namely OC, EC, ions (Na$^+$, NH$_4^+$, Mg^{2+}, Ca^{2+}, NO$_3^-$, SO$_4^{2-}$), trace metals (Al, Cu, Fe, Rb, Sb, Se, Sn, Ti, Zn) and organic markers (MSA, levoglucosan, polyols (sum of arabitol and mannitol)). We assumed that arabitol and mannitol came from a similar source and, hence, combined them into one component named as "polyols" (Samaké et al., 2019). The uncertainties of the input variables were calculated based on Gianini et al. (2012). Finally, the species displaying a signal-to-noise ratio (S/N) lower than 0.2 were discarded and those with S/N between 0.2 and 2 were classified as "weak", consequently multiplying the uncertainties by a factor 3.

2.4.2 Criteria for a valid solution

Solutions with a total number of factors from 6 to 11 were tested for the baseline models. Following the recommendations of the European guide on air pollution source apportionment with receptor models (Belis, 2019), a particular attention has been paid on the ratio Q$_{true}$/Q$_{robust}$ (< 1.5) and the weighted residuals. Moreover, the bootstrapping method (BS) was used on the final solution to estimate errors and ensure the stability and accuracy of the solutions. The BS method was applied with 100 iterations of the model.

2.4.3 Appropriate constraints in the PMF model

A set of constraints were applied on a basic model solution, in order to refine the results of the mathematical model by providing sound geochemical knowledge. Hence, the usual constraints as discussed in Weber et al. (2019) and some constraints corresponding to the traffic source following Charron et al. (2019) were also tested on the model (Table S2). However, these set of constraints were tested in caution as most of them have been previously applied only on sites with different typologies (i.e., urban or roadside sites), questioning their applicability in a rural site such as the OPE site. Finally, only a limited set was applied to generate the final solution (S1). After application of the constraints, a BS method was re-applied to verify the stability of the model.

2.4.4 Similarity assessment of chemical profiles

To investigate further any difference in the chemical profiles at the OPE site compared to those obtained at other French sites, a test of similarity was performed using the Pearson distance (PD) and standardized identity distance (SID) metric. This is calculated using Eq. S5 and Eq. S6 in the SI (S2) (Belis et al., 2015), closely following a previous work by our group (Weber et al., 2019). This comparison is based on the source relative mass composition, which allows the evaluation of the variability of solutions across different sites. In this case, the chemical profiles of the final PMF solution for the OPE site was compared against those at 15 different sites over France. A "homogenous source" tends to be stable over different site types and should have PD<0.4 and SID<1.0 (Pernigotti and Belis, 2018). Conversely, the factors outside of this range are considered as "heterogeneous sources".

2.5 OP source contribution estimation

The OP contribution of each PM_{10} source was determined by performing an OP deconvolution method using multiple linear regression (MLR) analysis. This method is based on previous reports on OP studies in France (Weber et al., 2018, 2021; Borlaza et al., 2021). Briefly, the OP activity in nmol/min/m³ was used as the dependent variable, while the PMF-resolved source PM_{10} mass contributions in μg/m³ are the independent variables, as shown in Eq. 1:

$$OP_{obs} = (G_n \times \beta_n) + \varepsilon, \tag{Eq. 1}$$

where OP_{obs} is the observed daily OP_v ($nmol_{reactant}$ min^{-1} m^{-3}) with matrix size d×1, G is the PMF-resolved source contribution (μg m^{-3}) of size d×n, and β is the regression coefficient representative of the intrinsic OP (OP_m) (nmol min^{-1} $μg^{-1}$) of each n source. Finally, ε is the residual between the observed and modeled OP ($nmol_{reactant}$ min^{-1} m^{-3}). The source-specific OP contribution is calculated by multiplying the regression coefficient of each source by the mass contribution of the source to PM_{10} ($G_k \times \beta_k$). This methodology is essentially based on that in Weber et al. (2018).

2.6 Season-trend (STL) deconvolution method

To investigate the long-term trends of sources or species concentrations, the STL (Season-trend deconvolution using locally estimated scatterplot smoothing) model (Cleveland et al., 1990) was applied on the monthly mean concentrations, as described by Eq. 2:

$$Y(t) = T(t) + S(t) + r(t) \tag{Eq. 2}$$

where : $Y(t)$ is the time series observed in monthly average, $T(t)$ is the trend component of the signal, $S(t)$ is the seasonal component, and $r(t)$ is the residual part not explained by the trend and seasonal part. The frequency was set to 13 (i.e., 6 months before and after the current month) to account for yearly seasonality. This model uses an iterative algorithm that constantly minimizes the residual $r(t)$ by successively adjusting the trend and seasonal components. It has to be noted that the resulting $T(t)$ and $S(t)$ do not represent concentrations, but a statistical deconvolution of the input signal $Y(t)$. $S(t)$ could then be negative and the trend $T(t)$ should be interpreted as an elaborated "moving average" of the concentrations.

To account for extreme events or outliers in the data, the impact of data points with very high residuals were given less weight in the estimation of the trend and seasonal components, using the "robust" option of the algorithm. The presence and strength of tendency was evaluated thanks to the ordinary least square (OLS) linear fit of the $T(t)$ component against time, removing the first and last 6 month of the time-series to avoid edge-effects. Note that due to the lack of PM_{10} measurements in July 2019, the concentrations for that month were arbitrarily set to the August 2019 values. This model was implemented in Python 3.8 making use of the *statsmodels* module (Seabold and Perktold, 2010).

3 Results and discussion

The sections 3.1 to 3.5 below discusses the concentrations, sources, and trends of PM_{10}, while the sections 3.6 and 3.7 discusses the OP measurements and sources.

3.1 PM_{10} and its major chemical components

The reconstructed mass of PM_{10} in the OPE site was calculated following Eq. S1 in the SI and is presented in Figure 2. The mass concentration of the reconstructed daily PM_{10} samples ranged from 2 to 51 µg m^{-3} with an overall average of 9 ± 7 µg m^{-3} (median: 8 µg m^{-3}). These reconstructed PM_{10} mass concentration only exceeded the PM_{10} European limit value of 40 µg m^{-3} a few times ($n = 3$) in the entire measurement period. These values are in the lower range of the concentrations reported for rural areas in Europe, ranging from 3 to 35 µg m^{-3} (Putaud et al., 2004), and are relatively close to the values found at a remote site in Revin (France, located 165 km away), as described in the SOURCES programme (average of 13 µg m^{-3}) (Weber et al., 2019). Although, there are minor variabilities observed in the yearly average of reconstructed PM_{10} from years 2012 to 2020, there are no notable drastic changes in PM_{10} mass concentrations nor in the major chemical components at the OPE site, even with the lockdown restrictions during year 2020.
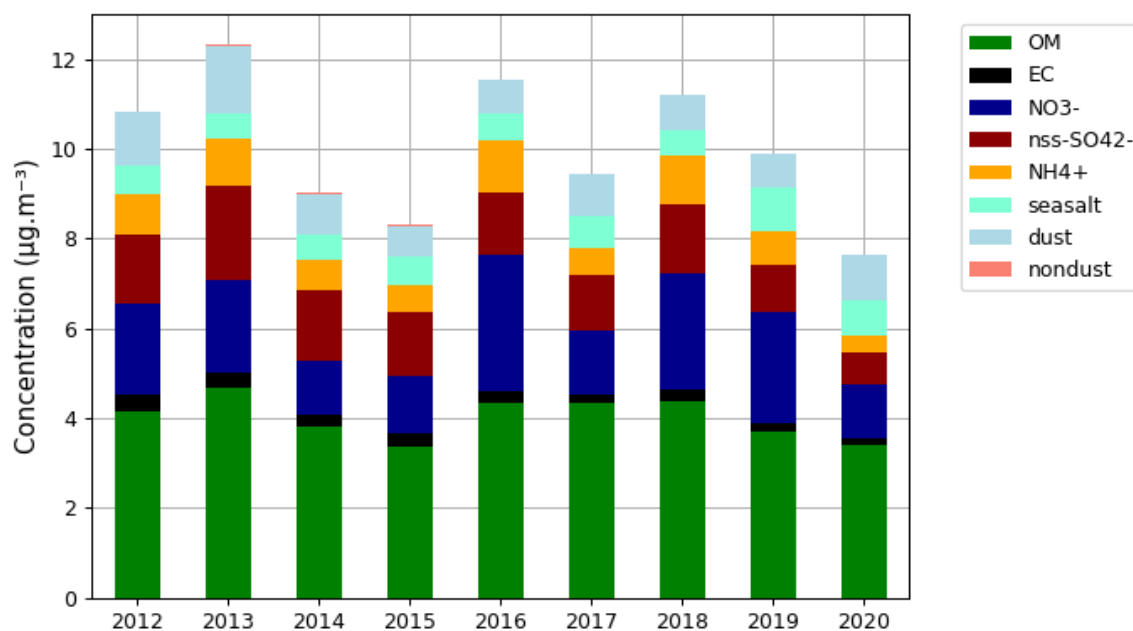
Figure 2: The annual average of PM_{10} composition in the OPE site.

Accounting for 39% of the reconstructed PM_{10} mass concentrations, organic matter (OM) is the largest contributor. The other main contributors are inorganic secondary species (NO$_3^-$, NH$_4^+$, nss-sulphate), suggesting a strong influence from LRT of pollutants. There are also contributions coming from dust and sea salt. Although all of these components are often dominated by specific emissions, they can be derived from a wide range of sources. For example, vehicular emissions are usually

composed of both carbonaceous and metals species, while road dust are usually minerals and some metal species.
220   Understanding the sources (as with the PMF methodology) and transformation processes of PM proves to be an essential step for efficient air quality policies.

3.2 Statistical stability of the PMF solution

The final retained solution includes 9 factors as described in section 3.3. Only 71 out of 100 baseline runs (without constraints) converged for this solution, but most factors were 100% correctly mapped, except for the traffic factor (93%, 66 out of 71
225   converged solutions) and sulphate-rich factor (99%, 70 out of 71 converged solutions). Applying the constraints greatly improved the BS mapping to 100% (100 out of 100) on all factors. Adding constraints in the base model allowed refining of the model through addition of expert knowledge on the profiles, which lead to the increased model stability. In previous source apportionment studies, specifically by our group, there are common constraints used depending on the site type such as presented in Borlaza et al. (2020).
230   Particularly, the constraints for traffic-related factors reported in Charron et al. (2019) have been optimized for traffic and urban background sites in our previous works. However, these constraints appeared restrictive when applied in a rural typology such as the OPE site. In fact, the Cu-to-Sb ratios appeared unsuitable as this ratio was 6.3 in our final solution compared to 12.6 in Charron et al. (2019). Based on literature, the Cu-to-Sb ratio can range from 1.6 (Handler et al., 2008) to 12.6 (Charron et al., 2019) depending on site typology. The addition of this constraint resulted in or led to a non-convergent solution in the
235   OPE site. To avoid inconsistencies, the Cu/Sb constraint was excluded in the optimal solution. The OC-to-EC ratio in the traffic profile was also too restrictive for the model, as this ratio was 3.9 in our baseline solution against 0.44 in Charron et al. (2019). The OC/EC levels calculated in this profile also suggests a strong influence of secondary organic aerosols (SOA) (Johnson et al., 2006; Pio et al., 2011; Rodríguez González et al., 2003; Viana et al., 2006), instead of primary traffic emissions. As OC in a rural site can undergo multiple re-transformations in the atmosphere, this can lead to a wide range of OC-to-EC
240   ratios as similarly found in Weber et al. (2019), hence this constraint was excluded.
In the final model, some constraints were used as summarized in Table S2, which resulted to all factors being correctly mapped and all BS runs converged, suggesting a good improvement in the traffic (from 93% to 100%) and sulphate-rich (from 99% to 100%) factors as well as the overall statistical robustness of the model. The other constraints either resulted in a non-convergent constrained model and/or less robust BS results. This implies that in sites with strong influence of LRT, the appropriate
245   constraints tend to vary and an optimal PMF solution can be more difficult to achieve.
The challenge in adding the constraints may also be linked to the inherent nature of the PMF algorithm since it assumes chemical profiles are identical for the whole period of analysis. However, during the 9 years of this study, some chemical source profiles may have changed, notably the traffic factor. Indeed, an evolution of the car fleet in France and Europe could lead to the changes in the OC-to-EC ratio emitted by the vehicle, so this profile may also have changed during this period. For
250   this specific case, a rolling PMF approach (Canonaco et al., 2021) with statistically-mapped PMF profile could be useful to investigate the time-variability of a given profile, slightly evolving with time.

3.3 PMF solution description and PM₁₀ contributions

The 9 resolved sources of PM$_{10}$ in the OPE site include nitrate-rich (25% of average contribution to PM$_{10}$ for the full period), sulphate-rich (15%), traffic (12%), mineral dust (16%), biomass burning (9%), fresh sea salt (4%), aged sea salt (6%), primary

255 biogenic (7%), and MSA-rich (7%). These factors were identified based on their chemical profiles and the mass loading of specific tracers, as summarised in Table S1 in the SI. The error estimations, chemical profiles, and temporal evolutions of the PMF-resolved sources are available in the SI (S3). Figure 3 represents the repartition of the chemical species in the different factors. The summed PM$_{10}$ contributions from all sources showed very good mass closure (r=0.95) with PM$_{10}$ mass reconstructed with Eq. S1, indicating very good model results.
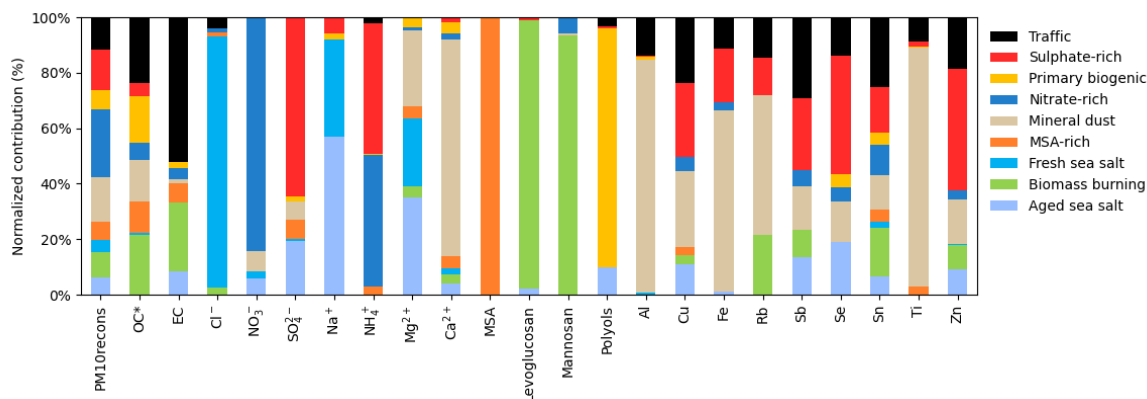
260

Figure 3: Species repartition by PMF-resolved sources in the OPE site.

The factors with highest average contribution to the PM$_{10}$ mass are the two inorganic secondary aerosol sources, nitrate-rich (25%, 2.3±4.3 µg m^{-3}) and sulphate-rich (15%, 1.4±1.5 µg m^{-3}), and mineral dust (16%, 1.6±1.7 µg m^{-3}). Sulphates and nitrates are mainly formed through secondary processes in the atmosphere with long atmospheric lifetimes and can, therefore, originate

265 from regional sources or LRT. The less dominant sources are traffic, biomass burning, biogenic (MSA-rich, primary biogenic), and sea salts (fresh and aged). The contributions of the different factors are quite similar to those observed at other rural sites in France (Weber et al., 2019).

The OPE site has a Northern hemisphere mid-latitude climate with four seasons, (1) winter season corresponding to the months of December, January, February; (2) spring season corresponding to March, April, May; (3) summer season corresponding to

270 June, July and August; and (4) fall season corresponding to September, October and November. Seasonality in some factors can be apparent, such as for the biomass burning and nitrate-rich factors, which are more prominent in winter and spring, respectively, and the primary biogenic and MSA-rich factors, increasing in summer due to greater photochemical and biological activities. Figure 4 depicts the seasonal average contributions of the PM$_{10}$ sources at the OPE site from years 2012 to 2020.

275 The **nitrate-rich** factor, identified by high loadings of NO_3^- and NH_4^+, has a strong seasonal pattern with maximum contribution to PM_{10} mass concentration especially in the months of March and April. The NH_4^+/NO_3^- mass ratio in this factor is 0.22, close to the mass ratio (0.29) indicating the formation of NO_3NH_4 in the particulate phase.

The **sulphate-rich** factor is identified by high loadings of SO_4^{2-} and NH_4^+. There are also contributions from some metal species (Se, Zn, Cu, and Sb) in this factor, suggesting potential influence from road dust and/or non-tail pipe vehicular

280 emissions. A small portion of OC (5% of OC mass) is also observed in this factor. The presence of these metals remained, even when the number of factors were increased (up to 11 factors) during the PMF optimization process. The NH_4^+ to SO_4^{2-} molar ratio of 0.4 suggests that sulphates are mostly present as $(NH_4)HSO_4$ and only a small fraction as $(NH_4)_2SO_4$.

The **aged sea salt** factor is characterised by high loadings of Na^+ and Mg^{2+}, with a certain amount of species originating from potentially anthropogenic sources such as nitrates (6% of NO_3^- mass) and sulphates (19% of SO_4^{2-} mass) that can be attributed

285 to mixing and transformation processes in the atmosphere. Interestingly, there are some contributions from EC (8% of EC mass), Cu (11% of Cu mass), Sb (13% of Sb mass), and Se (19% of Se mass). This could imply potential mixing of aged sea salt with other anthropogenic source linked to these species (e.g., traffic, shipping). There was no added constraint in this factor as our solution shows a Mg^{2+} to Na^+ ratio at 0.06 while this ratio is usually found around 0.12 in sea-salt emissions (Henderson and Henderson, 2010).
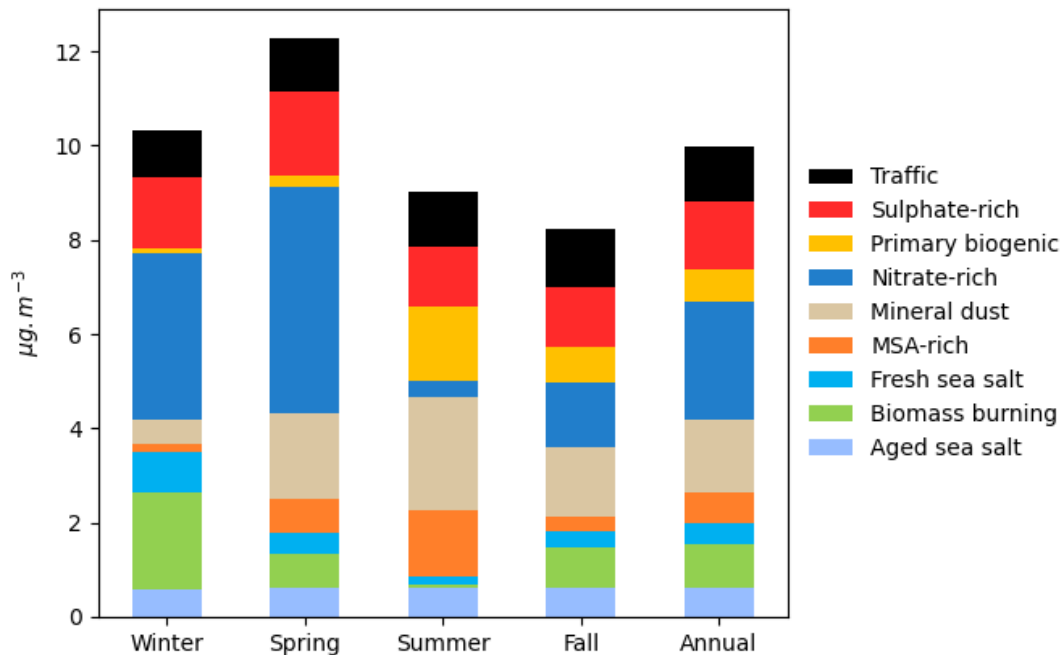
290

Figure 4: Seasonal and annual contribution of the PMF-resolved sources in the OPE site.

The **MSA-rich** factor identified by high loadings of MSA (methanesulfonic acid), a known product of oxidation of dimethylsulfide (DMS) commonly from marine phytoplankton emissions (Chen et al., 2018; Li et al., 1993). A small mass fraction of SO_4^{2-} (7% of SO_4^{2-} mass) is also found in this factor, that may be due to the co-emission of DMS and non-sea salt

295   sulphates, but also resulting from the production of biogenic sulphate from DMS oxidation. Hence, MSA-rich could potentially
       be mixed with secondary inorganic aerosols as well. The measured MSA mass concentration showed weak correlations with
       specific ionic species from marine aerosols such as Na^+ ($r<0.01$) and Mg^{2+} ($r<0.01$). This could indicate that marine biogenic
       emissions may not be the only source of this factor. Instead, this factor could be influenced by sources with terrestrial origins
       and/or from forest biota, as previously reported in other studies (Bozzetti et al., 2017; Golly et al., 2019; Jardine et al., 2015;

300   Miyazaki et al., 2012). This factor also presents a clear seasonal pattern with maximum contribution from May to July due to
       higher photochemical activity and algae / microbial activity. Golly et al. (2019) reported a very coherent seasonal cycle for
       MSA concentrations over a large portion of the French territory, including at the OPE site.

       The **primary biogenic** factor is characterised entirely by polyols. These species are emitted by fungal spores which partly
       explains the high loadings of OC found in this factor. This factor has a higher contribution to PM_{10} during the summer season,

305   consistent with the observations at other rural and urban typologies (Samaké et al., 2019; Weber et al., 2019; Borlaza et al.,
       2021). More details about the characteristics of primary biogenic aerosols can be found in Samaké et al. (2019). Briefly,
       meteorological conditions, such as high temperature and relative humidity, could facilitate the increase in their formation. This
       factor can also include some fraction of plant debris, identified by cellulose measurements, as discussed in Samaké et al.
       (2019), Borlaza et al. (2021), and Brighty et al. (2021).

310   The **biomass burning** factor, a major contributor to PM_{10} during the winter season, includes most of levoglucosan and
       mannosan. This factor contains around 25% of the total EC mass, consistent with a combustion chemical profile. Trace
       elements like Rb and Sn are also found in this factor, rubidium being the major trace element with 21% of its mass being
       reconstructed in this factor. Due to the distance of any residential areas from the OPE site, the contributions of this factor to
       PM_{10} at 20% on winter average is much less than the contributions generally observed in most sites in France in winter (e.g.,

315   urban, sub-urban or countryside sites), which are mainly in the range of 25 - 70 % with an average of about 35% (Weber et
       al., 2019). The contribution at the OPE site most probably represents the average winter loading of the French national
       background of the atmosphere.

       The **traffic** factor is the second factor where EC is a major contributor (52% of EC mass). The major trace elements found in
       the traffic factor are Cu, Sb, Sn, and Zn, and most of their masses are reconstructed in this factor. There is no seasonality

320   associated with this factor. However, its contribution to PM_{10} presents a decreasing trend over the sampling period from 2012
       to 2020. This is also consistent with the decreasing trend found in EC mass concentrations over the same period, as presented
       in Figure S11. These findings present an opportunity to explore the potential decrease in traffic emissions observed in the OPE
       site, taken as a good proxy of the national background burden of the rural atmosphere. This is further discussed in section 3.5.

       The **mineral dust** factor is mainly composed of Ca^{2+} (78% of Ca^{2+} mass), Al (84% of Al mass), and Ti (86% of Ti mass).

325   There are also contributions from other trace elements that could be originating from re-suspended road dust or non-tail pipe
       emissions such as Fe (65% of Fe mass), Cu (27% of Cu mass), Rb (51% of Rb mass), and Zn (16% of Zn mass). A fraction of
       it could therefore be of anthropogenic origin.

3.4 Comparison of source chemical profiles in the SOURCES programme

Figure 5 presents the similarity plot (PD-SID distances) obtained for the 9 factors found in the OPE site compared to the French

330   sites included in the SOURCES programme (Weber et al., 2019). It is striking that most factors remained homogeneous within

France, including both rural and urban sites. The most stable factors are nitrate-rich (lowest PD) and mineral dust (lowest SID).

The traffic factor also appears relatively stable, but presents some dissimilarity according to the high variation in the PD metric.

A high PD variation generally indicates a difference in the chemical species that identify the main mass contribution of the

profile. In fact, in the traffic factor, this variation between the OPE and other sites can be attributed to the variations in the OC

335   to EC levels, similar to the findings in Weber et al. (2019). Compared to the other French sites, the OC to EC levels of this

factor in the OPE site are much higher, which highlights a strong influence from LRT processes with SOA formation.

The aged sea salt and MSA-rich factors are the only ones positioned outside of the shaded box in Figure 5, indicative of

heterogeneous profiles between the OPE and the other sites. The heterogeneity found in the aged sea salt profile can be

attributed to the contributions of EC and some metals in this factor. These were not typically found in other sites in France and

340   could also be due to the mixing of this sea salt profile with other anthropogenic contributions as a result of LRT processes, as

well as different aging processes. Similarly, the MSA-rich factor has previously shown site-to-site variations and a wide

variation in the PD-SID metric (Weber et al., 2019), mostly attributed to the variability of the contribution of OC in some sites.

This is also the case in the OPE site, with a large contribution of about 11% of OC in this MSA-rich factor. Despite these few

differences, the very large similarity of the chemical profiles at OPE compared to those at all other sites in France will be

345   essential to the comparison of the intrinsic OP of sources in section 3.7.
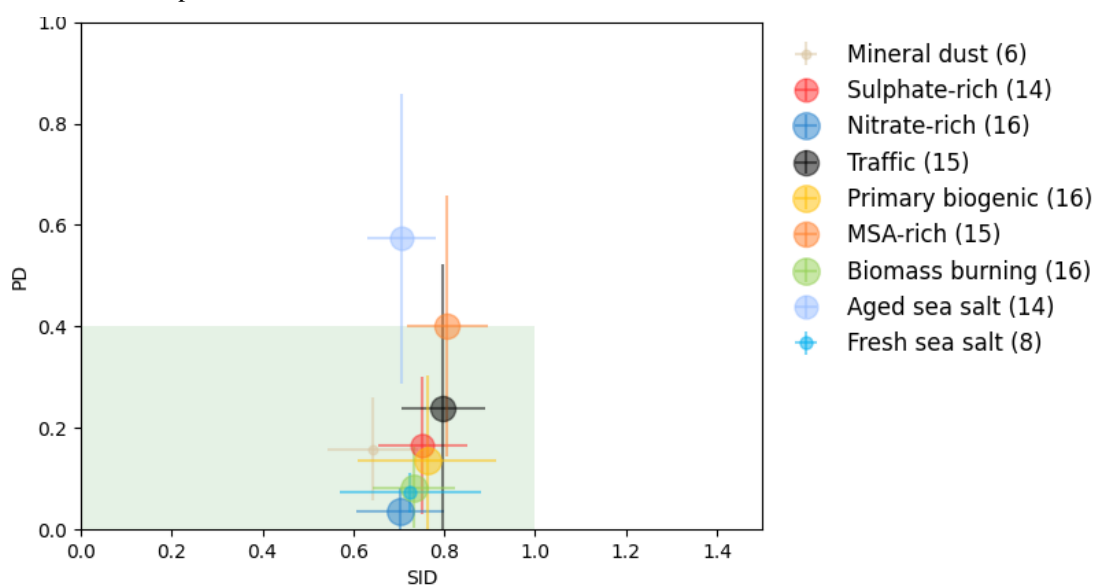
Figure 5: Similarity plot of the OPE site against all the French sites in the SOURCES programme. The shaded area (in green) shows the acceptable range of the PD-SID metric. For each point, the error bars represent the standard deviation in the comparisons of all pairs of sites. The number in the legend indicate the number of sites over France were the given profile is available.

3.5 Long-term trends of PM$_{10}$ sources

Figure S10 in the SI presents the long-term trend of the observed PM$_{10}$ in the OPE site. The PM$_{10}$ levels appear to be consistent from 2012 to 2020 and there is no clear increasing or decreasing trend found in PM$_{10}$ (r^2=0.2, Table 1). However, there is a clear decline found in EC mass concentrations (r^2=0.9) with a reduction of 22 ng m^{-3} year^{-1} ($p\leq0.01$) (Figure S11 in the SI). This could indicate that the mass contribution of one or more sources contributing to EC should also be decreasing. Following Germany and Italy, France places third on highly impacted countries in Europe from vehicular exhaust emissions (Anenberg et al., 2010). Through the years, a variety of vehicular regulations have been adopted to reduce traffic-related emissions, not only in France (Bernard et al., 2020), but also across Europe (Wappelhorst and Muncrief, 2019). The data obtained in the OPE site poses an interesting opportunity as it covers 9 years of sampling in a rural area, making it possible to investigate emission trends over a long period of time in a site representing a background atmosphere.

Using the model described in section 2.6 (Eq. 2), the STL deconvolution of the PMF-resolved sources in the OPE site were also investigated. It is extremely significant that the contributions from the traffic factor in the OPE site also decreased substantially, as presented in Figure 6. A very large reduction of 58% from year 2012 to 2020 based on average mass contribution and an overall yearly average reduction of 104 ng m^{-3} y^{-1} ($p\leq0.01$) were found. In parallel, there is also a reduction observed in the sulphate-rich factor, proposed as a highly anthropogenic-derived factor (see Figure S11 in the SI), with 66% reduction of average mass contribution and an over-all yearly average reduction of 72 ng m^{-3} y^{-1} ($p\leq0.01$). Indeed, several other sources have shown lower but significant decrease of their mass contribution over the years (Table 1) in the OPE site, except for the fresh sea salt, nitrate-rich, and MSA-rich factors.

Table 1: STL tendencies of the observed PM$_{10}$ and each PMF-resolved source contributions to PM$_{10}$ from year 2012 to 2020 in the OPE site.

	Tendency (µg m^{-3} year^{-1})	r^2	p-value
Observed PM$_{10}$	-0.107	0.21	≤0.01
EC	-0.022	0.89	≤0.01
Traffic	-0.104	0.67	≤0.01
Aged sea salt	-0.042	0.52	≤0.01
Fresh sea salt	0.052	0.77	≤0.01
Mineral dust	-0.055	0.09	≤0.01
MSA-rich	0.013	0.14	≤0.01
Nitrate-rich	-0.002	0.00	0.90
Primary biogenic	-0.027	0.82	≤0.01
Sulphate-rich	-0.072	0.57	≤0.01
Biomass burning	-0.033	0.64	≤0.01

The downward trends found in our study are well consistent with other existing studies in Europe (Li et al., 2018; Sun et al., 2020; Salvador et al., 2012; Pandolfi et al., 2016; Gama et al., 2018; Amato et al., 2014). Pandolfi et al. (2016) found a significant long-term decrease of the contributions from anthropogenic emissions (specifically industrial/traffic, -0.11 µg m^{-3} year^{-1}, 56% total reduction) in a regional background site in northeast of Spain (Montseny, Spain) from 2004 to 2014. This is

375 also consistent with a similar study in the metropolitan area of Madrid, Spain (Salvador et al., 2012) which showed a reduction of 32.7% attributed to traffic emissions, alongside the decrease of the carbonaceous and SO_4^{2-} in PM. In a southern Spain area (Andalusia), the same group also found a consistent decreasing trend of PM at some traffic and urban sites in the region (Amato et al., 2014). Another long-term study in Central Europe (Sun et al., 2020) focusing on eBC concentrations found decreasing trends in high-Alpine sites located in Germany (-3.88% year[-1], [-10.15%, 0.56%]) and Switzerland (-3.36% year[-1], [-8.71%, -

380 0.28%]). These findings are also consistent with results from other parts of Europe (Cusack et al., 2012), with the largest decrease found in OC up to -48%. Most of these studies were conducted in urban areas, and attribute this decline in species or sources to the targeted efforts to reduce vehicular emissions and other mitigation policies.

The interesting points of our study is that it pertains directly to a specific source, identified with a long term and robust PMF study. Further, as there are minimal local anthropogenic sources expected in the OPE site, it may be safe to assume that these

385 contributions to PM mass in this area are influenced by LRT of pollutants. Our results indicate that the implementation of emission control policies are also playing a role in the consistent decrease in traffic emissions in rural sites far away from direct emissions.
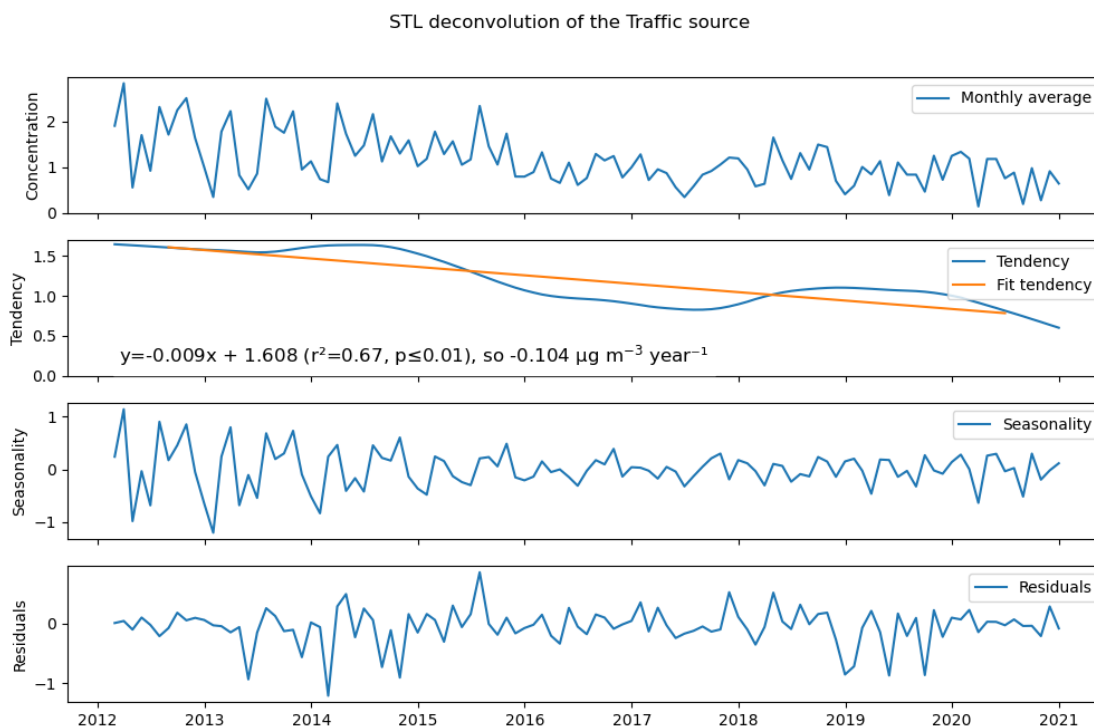
Figure 6: The Season-trend (STL) deconvolution of contributions from the traffic factor to PM$_{10}$ from year 2012 to 2020.

3.6 Temporal trends of observed OP of PM$_{10}$

Figure 7 presents the observed average values of OP of PM$_{10}$ in the OPE site compared to the other sites in France (Calas et al., 2018, 2019; Weber et al., 2021, 2018). All series cover at least one year of sampling. As expected, the OP level in a rural background is much lower (about 2 to 8 times) than other typologies including traffic, urban, and urban alpine sites, for both AA and DTT assays. Further, the average ratio between urban sites and the rural OPE site is generally much higher for OP's than for PM mass, an indication that the nature of the particles at the rural site make them less oxidant than in urban areas, as already pointed out in Daellenbach et al. (2020).

Figure 8 presents the daily and monthly mean distributions of observed PM$_{10}$ and OP activity (OP_v^{DTT} and OP_v^{AA}) from June 13, 2017 to December 22, 2020. There is an observed seasonality, where PM$_{10}$ and OP_v^{DTT} appear to be similar with relatively higher levels during warmer months. On the contrary, OP_v^{AA} has slightly higher levels during colder months.

In many European studies, the seasonality in PM$_{10}$ mass concentration can be usually explained by higher contributions from biomass burning during winter (Bessagnet et al., 2020; Tomaz et al., 2017), especially in alpine valleys (Calas et al., 2019b; Favez et al., 2010; Herich et al., 2014; Srivastava et al., 2018; Tomaz et al., 2016, 2017; Weber et al., 2018, 2019; Borlaza et al., 2021). Similarly, this seasonal pattern has been observed in OP as well (Borlaza et al., 2021; Weber et al., 2018; Calas et al., 2019b; Weber et al., 2021). However, the typology (i.e., rural) of OPE site could be associated with a different type of OP temporal profile as it is far from direct anthropogenic emission sources (but not from vegetation and soil biogenic emissions).
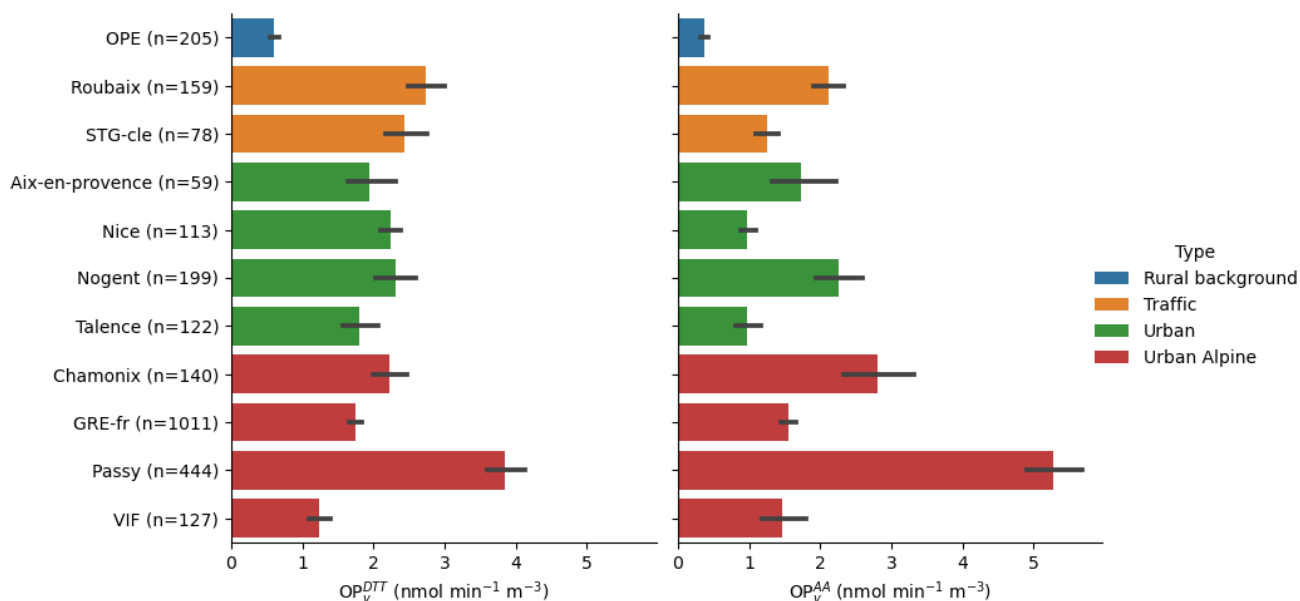
Figure 7: The comparison of observed OP activity (OP_v^{DTT} and OP_v^{AA}) between the OPE site and other sites in France. Bar plots depict the mean value with standard deviation.

With the large influence of LRT on the sources of PM in the OPE site, this also poses an opportunity to investigate on the impact of LRT on OP. In fact, few studies have looked into the effects of aerosol aging to OP properties (Guascito et al., 2021;

Bates et al., 2019). Pietrogrande et al. (2019) reported association of OP to redox-active organics linked to photo-oxidative aging. Using backward trajectory analysis, Wang et al. (2020) found strong effects of LRT on OP of fine PM. This is also consistent with the findings in Paraskevopoulou et al. (2019) which revealed highly oxygenated secondary aerosols as one of the main drivers of OP in fine PM, further highlighting the importance of combustion and aging processes in OP. In a shipborne

415 measurement study in South Korea, a higher intrinsic OP has also been found in samples where secondary aerosol formation is more dominant, also suggesting strong impacts of long-range transported PM (Oh et al., 2021). Cesari et al. (2019) found negligible contribution from secondary sulphates, but have found relevant OP contributions from a factor identified as a combination of vehicular traffic and secondary nitrates. All these studies used DTT assay to measure the OP of PM.

The OP assay sensitivity to specific species and/or sources can also explain the difference in seasonality found in OP_v^{DTT} and

420 OP_v^{AA} in our study. OP_v^{DTT} appears sensitive towards organics, metals, and, possibly, a synergistic effect between the two (Bates et al., 2019; Dou et al., 2015; Fang et al., 2017; Gao et al., 2020b, a; Jiang et al., 2019; Weber et al., 2021; Yu et al., 2018; Borlaza et al., 2021), while, OP_v^{AA} shows sensitivity mostly towards metal species (Bates et al., 2019; Crobeddu et al., 2017; Visentin et al., 2016; Weber et al., 2021; Borlaza et al., 2021).

Generally, current literature poses importance of the role of secondary/aged aerosols on OP of PM, especially those with

425 influence from anthropogenic sources. However, to our knowledge, this is the first long-term OP study, especially dealing with ambient samples far from direct emissions at a rural background site.

3.7 Sources of OP in PM$_{10}$

The sources of OP in PM$_{10}$ was apportioned following an OP deconvolution method proposed by Weber et al. (2018) using the source contributions (μg m^{-3}) obtained in the PMF and the measured OP (nmol min^{-1} m^{-3}) at the OPE site. Generally, the

430 modelled OP (OP_m) is within range of the observed OP, with a reasonable reconstruction (OP_v^{DTT} (r=0.76) and OP_v^{AA} (r=0.76)). The OP_m of each PM source is given in Table 2, where OP_m^{DTT} can range from -0.01±0.02 to 0.10±0.03 nmol min^{-1} μg^{-1} and OP_m^{AA} can range from -0.001±0.02 to 0.16±0.03 nmol min^{-1} μg^{-1}. Generally, higher OP_m indicates higher redox-activity associated with the factor. There are some differences in the OP_m based on the type of assay used and this can be attributed to the sensitivity of the assay towards certain redox-active species in PM (Borlaza et al., 2021; Xiong et al., 2017; Charrier and

435 Anastasio, 2012).

In terms of overall daily mean contribution, as presented in Figure 9, the main contributors to PM$_{10}$ mass are the nitrate-rich, mineral dust, and sulphate-rich factors in the OPE site. However, in terms of OP_v^{DTT}, the mineral dust factor showed the highest average contribution (0.15 nmol min^{-1} m^{-3}), followed by the sulphate-rich (0.11 nmol min^{-1} m^{-3}) and traffic (0.07 nmol min^{-1} m^{-3}) factors. For OP_v^{AA}, the biomass burning factor showed the highest contribution (0.12 nmol min^{-1} m^{-3}),

440 followed by the traffic (0.07 nmol min^{-1} m^{-3}) and nitrate-rich (0.06 nmol min^{-1} m^{-3}) factors.
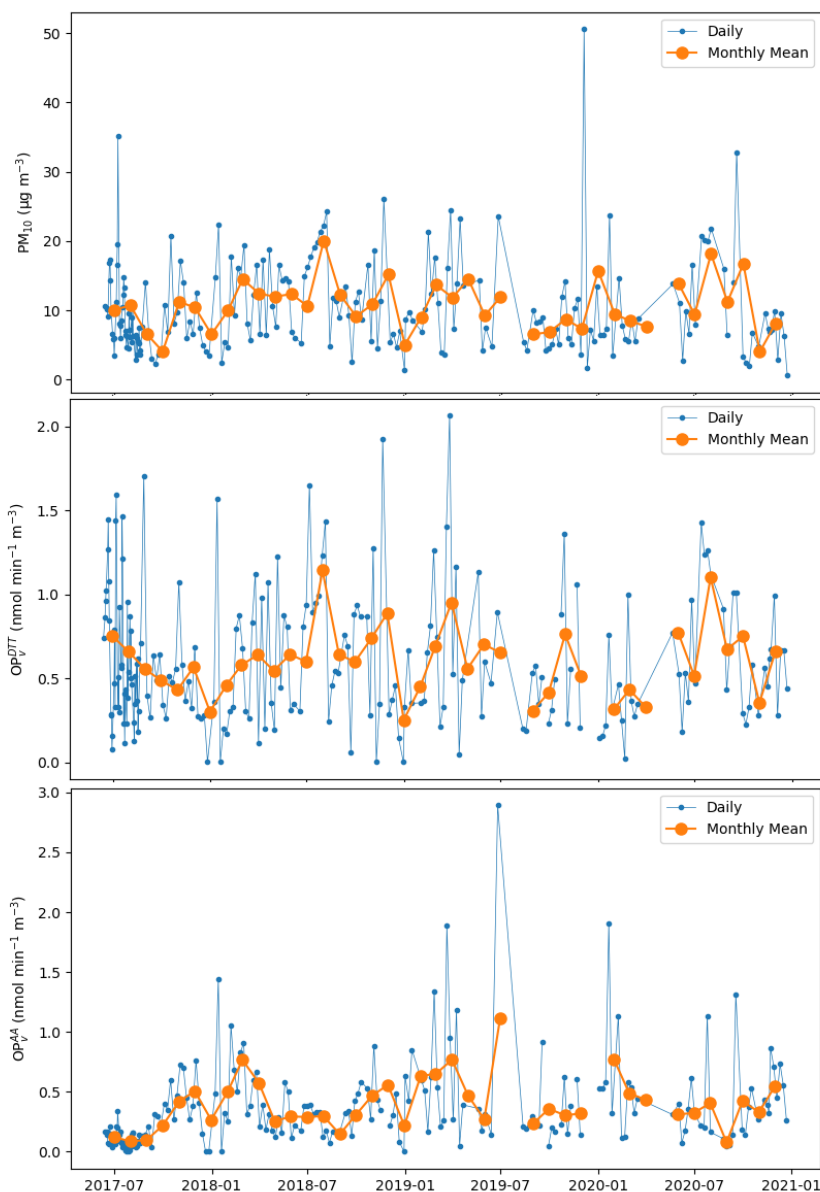
Figure 8: Temporal distributions of observed PM₁₀ and OP activity (OP_v^{DTT} and OP_v^{AA}) from year 2017 to 2020 in the OPE site in terms of daily and monthly mean.

Although lower in magnitude, the OP contribution of mineral dust, traffic, and biomass burning (only in OP_v^{AA}) are also prominent in the OPE site, similar to other sites in France (Weber et al., 2021). These sources are commonly composed of species that are highly redox-active, hence it is not surprising that they are one of the main drivers of OP even in a rural site. Both mineral dust and biomass burning are also sources that can be associated with LRT and aging, respectively, which are atmospheric processes linked to increased OP (Pietrogrande et al., 2019; Wang et al., 2020; Paraskevopoulou et al., 2019; Oh

et al., 2021). Further, while the mineral dust profile in OPE is considered homogeneous with those determined in other parts
450   of France, as discussed above, its chemical composition includes slightly larger fractions of some metals, particularly Fe and
Cu, possibly making it more redox-active.

Table 2: Regression coefficients (i.e., intrinsic OP or OP_m) expressed in nmol min^{-1} μg^{-1} at the OPE site for the DTT and AA assays. The values are the mean ± standard deviation and the p-value is in the parenthesis.

Factor	OP_m^{DTT}	OP_m^{AA}
Traffic	0.07±0.04 (p=0.09)	0.08±0.01 (p≤0.01)
Aged sea salt	0.06±0.04 (p=0.20)	0.08±0.04 (p≤0.05)
Fresh sea salt	0.02±0.02 (p=0.40)	0.02±0.02 (p=0.22)
Mineral dust	0.10±0.03 (p≤0.01)	0.04±0.01 (p≤0.01)
MSA-rich	0.04±0.04 (p=0.21)	-0.06±0.03 (p=0.06)
Nitrate-rich	0.01±0.01 (p=0.10)	0.03±0.01 (p≤0.01)
Primary biogenic	-0.01±0.02 (p=0.68)	-0.005±0.01 (p=0.82)
Sulphate-rich	0.10±0.03 (p≤0.01)	-0.001±0.02 (p=0.98)
Biomass burning	0.03±0.03 (p=0.42)	0.16±0.03 (p≤0.01)
Intercept (nmol min^{-1} m^{-3})	*0.14±0.06 (p≤0.05)*	*0.07±0.05 (p=0.16)*

455   As observed in other studies (Daellenbach et al., 2020; Borlaza et al., 2021; Weber et al., 2021), there is also a clear difference
in source impacts when considering the mass concentrations or the OP activity, highlighting the importance of redox activity
of inhalable particles as a metric of exposure. The mass contributions of the nitrate-rich factor can be twice as much as that of
the traffic factor. However, in terms of OP (both OP_v^{DTT} and OP_v^{AA}), the traffic factor contribution can be twice as much as that
of the nitrate-rich factor. The biomass burning factor, with only <1 μg m^{-3} mass contribution on annual average, appears to
460   have the highest contribution in OP_v^{AA}.

Some previous studies associated secondary inorganic sources (SIA) with minimal contributions on PM toxicity (Cassee et al.,
2013; Daellenbach et al., 2020; Park et al., 2018). However, the nitrate-rich factor apportioned in the OPE site showed
contributions to both OP_v^{DTT} and OP_v^{AA}, and the sulphate-rich factor to OP_v^{DTT}. In the sulphate-rich factor, a fraction of OC
(5%) and metals (Se (42%), Zn (44%), Cu (27%), and Sb (25%)) were apportioned, while in the nitrate-rich factor there are
465   contributions from OC (6%), EC (4%), and metals (Sb (6%) and Sn (11%)). These species are commonly anthropogenic-
derived, signalling that the sulphate- and nitrate-rich factors could be influenced by these types of emissions as well. In fact, a
similar study considered that both SIA factors can be associated to anthropogenic SOA sources (Borlaza et al., 2020).

Although both DTT and AA assays represent potential PM-induced oxidative stress, through in vivo interactions between
redox active components in PM$_{10}$ and biological oxidants, it can be observed that they differ in terms of source impacts. This
470   can be attributed to the sensitivity of each assay to specific species and/or emission sources of PM. Nevertheless, most of the
sources of PM suggested to be anthropogenic-derived or impacted, such as traffic, mineral dust, nitrate-rich, sulphate-rich
(only in OP_v^{DTT}), and biomass burning (only in OP_v^{AA}), were all usually in upper half of the scale (Figure 9) in terms of OP_v
contributions. The knowledge of source-specific OP_v contributions provide useful information on the main drivers of OP_v,
even in a rural area such as the OPE site.

475 There is an interesting seasonality observed in the OP of PM, as previously shown in **Erreur ! Source du renvoi introuvable.**. With the OP source deconvolution method, this seasonality has been revealed in terms of PM sources, as presented Figure 10. During colder months, the biomass burning factor clearly dominated the OP_v^{AA} contributions. During warmer months, the OP_v^{DTT} contributions were dominated by the mineral dust factor. However, there is a relatively consistent monthly contribution for both assays coming from the traffic factor.
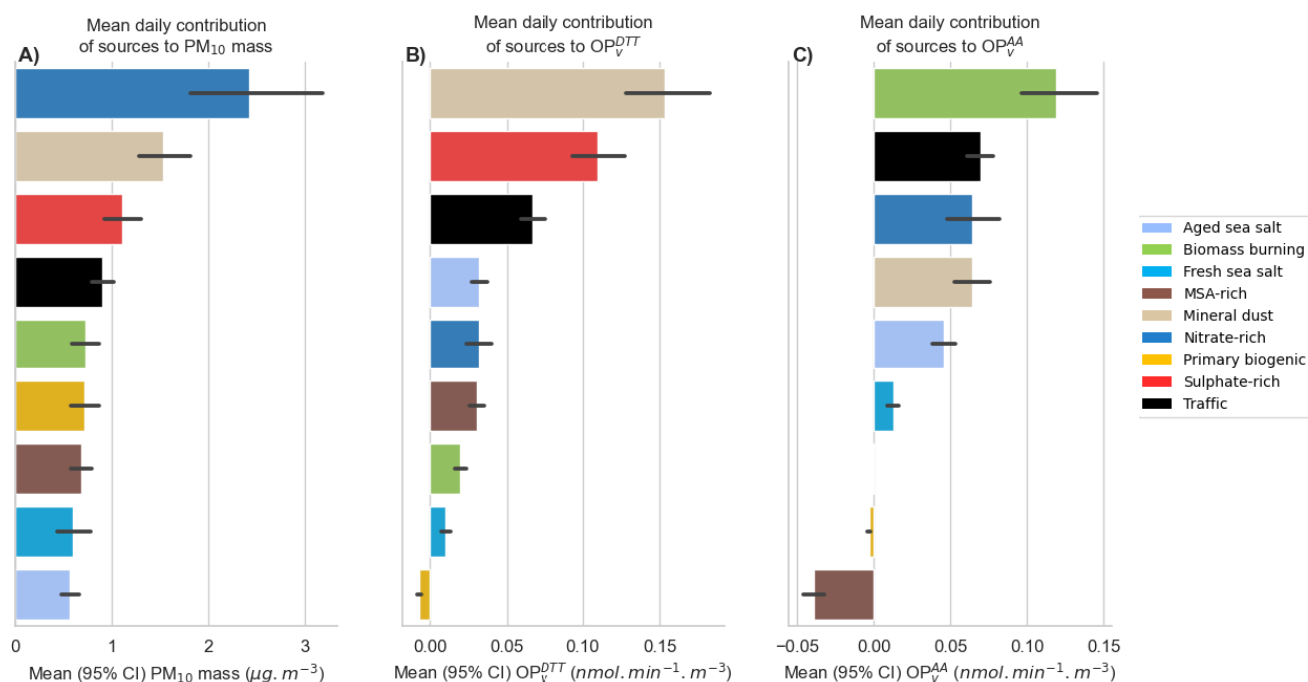
480

Figure 9: Overall daily mean OP_v contribution of the sources to PM₁₀ and OP activity (OP_v^{DTT} and OP_v^{AA}) using MLR analysis in the form of mean and 95% confident interval of the mean (error bar) (n=168 samples).

It is also interesting to note the negative contributions from some sources. This negative contribution is brought by a negative intrinsic OP (OP_m obtained in the OP deconvolution method (Table 2)). This can be broadly interpreted as follow: for every 1

485 µg m⁻³ increase in the MSA-rich factor, there is an associated decrease in OP_v^{AA} contributions (OP_m=-0.06±0.03, p=0.06). A similar interpretation can be done for the primary biogenic factor and its OP_v^{DTT} contributions (OP_m=-0.01±0.02, p=0.68). However, it is important to note that both MSA-rich and primary biogenic factors do not always present a negative OP_m in every site investigated in our group. One cannot completely assume that these two factors always act as suppressors of OP of PM. In fact, these two factors have shown high OP_m variabilities across different sites in France (Weber et al., 2021). With the

490 use of fit-for-purpose organic tracers, possible mixing issues in these factors can be minimized (Borlaza et al., 2021). However, these supplementary tracers were not available in the OPE site, making it difficult to eliminate potential influence from other factors or species in PM.
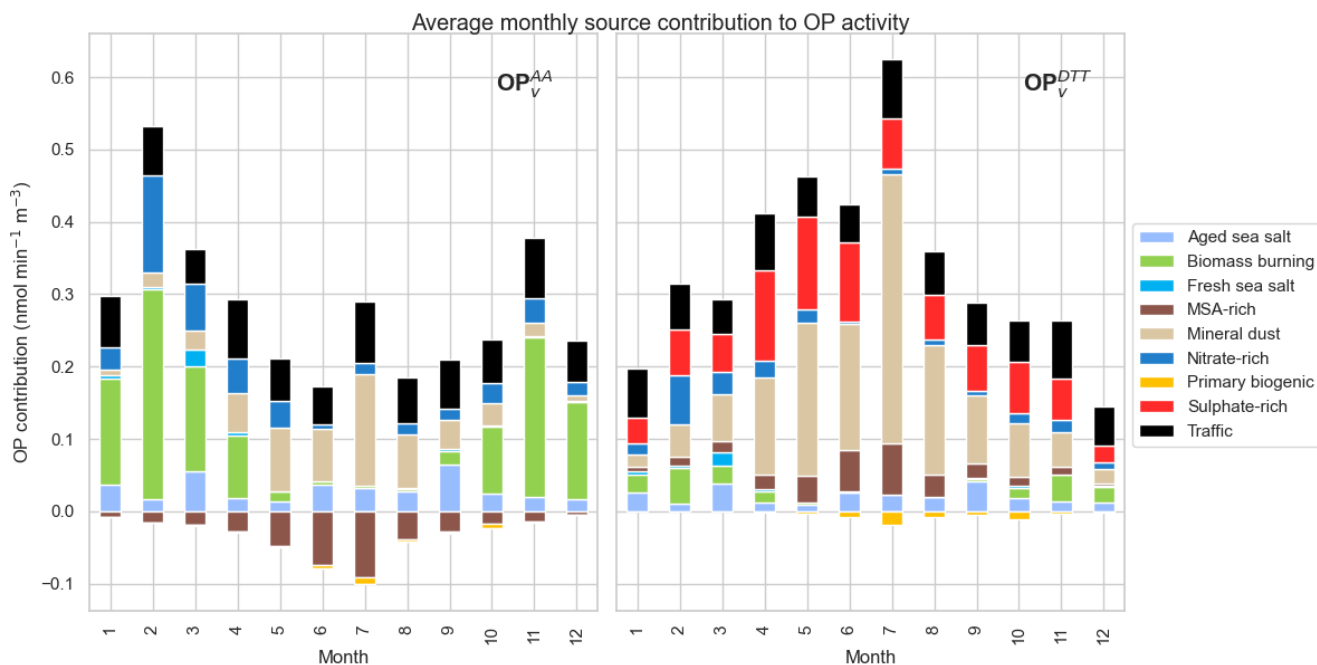
Figure 10: Monthly contribution of sources to OP activity in nmol min^{-1} m^{-3} (OP_v^{DTT} and OP_v^{AA}) from year 2017 to 2020 in the OPE site. Note: The months are labelled from January (1) to December (12).

Figure 11 presents the yearly contribution of each factor to the OP of PM$_{10}$ for the 3 years investigated in this study. There is no clear decreasing trend in the total OP reconstructed by MLR analysis. Although there is a decreasing trend found in the mass contributions of the traffic factor, this was not clearly reflected in its OP contributions. The other sources seem to have comparatively consistent OP contributions from 2017 to 2020, and no notable tendency can be found in the total OP contribution as opposed to the contributions to PM$_{10}$ mass showing decreasing trends. This may be explained by the limited subset of samples for the OP assay (OP data spanning 4 years against 9 years for the PMF data), the shorter time range being insufficient to reach significance and robustness in the trend assessment of OP levels.
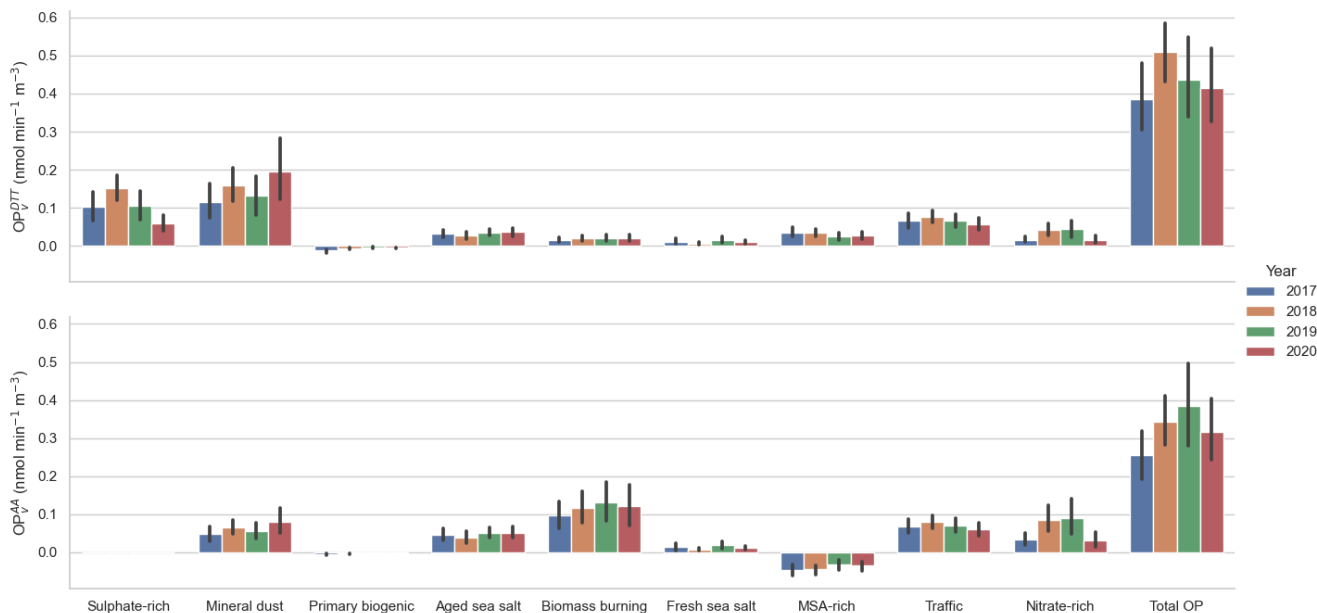
Figure 11: Yearly average contributions of sources to OP activity in nmol min^{-1} m^{-3} (OP_v^{DTT} and OP_v^{AA}) from year 2017 to 2020 in the OPE site. Note: Total OP is the sum of OP contributions of all sources as modelled by the MLR analysis.

3.8 Limitations of the study

In spite of the advantages offered by the long-term monitoring in the OPE site, there were a few limitations encountered during the investigation of the dataset. Each limitation is discussed as follows:

- There was a change in sampling duration between the 2012 to 2016 (7-day sampling) and 2016 to 2020 (24-hour sampling). A weekly sample includes both weekdays and weekends, whereas a daily sample will either be a weekday or weekend, depending on the sampling interval. This implies that the weekly collected samples may contain particles that are not fully captured in a daily sample. However, since the OPE site is quite distant from direct emissions, the expected difference in the weekday and weekend levels should be relatively small. Further, specific PMF were also conducted separately with each data sets, leading to very similar results for the chemical profiles and source contributions, justifying the coupled analysis. (see SI, Table S3 and Figures S12 to S20)

- The lack of fit-for-purpose tracers to fully elucidate the influence of SOA in a site with relevant distance from direct emissions (or rural typology) such as OPE. In Borlaza et al. (2021), a secondary biogenic oxidation source was additionally identified using organic tracers (3-MBTCA and pinic acid), while anthropogenic influence was supported by contributions of phthalic acid, even in secondary aerosol sources. With the typology in the OPE site, this would have been useful.

- The use of a single chemical profile for long-term PM source apportionment could be limiting for the PMF model. As we have found consistent decrease in some species, particularly EC, perhaps a rolling PMF (e.g., yearly PMF) could better capture possible changes in the source profiles.

525
- The absence of samples for OP analysis from years prior to 2017 have limited the investigation of long-term OP in the OPE site. Consequently, it was not easy to capture the decrease in OP contributions from the traffic factor as similarly captured in the mass contributions. Perhaps a hindcasting method on the years without OP data could have been performed, however that would heavily rely on the OP_m modelled from years 2017 to 2020, which can lead to bias in the results.

530
- In the year 2020, a series of lockdown restrictions were placed nationally as a response to the coronavirus disease (COVID-19) pandemic. In the OPE site, there is no clear decrease in average PM_{10} mass concentration in 2020 (Figure 11) that could have greatly affected the results of this study. In fact, excluding all samples from year 2020, the traffic factor contributions to PM_{10} still has a reduction of 39% from year 2012 to 2019 and an overall yearly average reduction of 135 ng m^{-3} y^{-1} ($p \leq 0.01$).

4 Conclusions

535   Over the 9-year analysis in a rural background site in France (OPE), the observed PM_{10} mass concentration and OP were found to be much lower than other sites in France. The sources of PM_{10} mass and OP were apportioned using PMF and MLR analysis, respectively. The nine identified factors relevant for PM_{10} include secondary inorganics (nitrate- and sulphate-rich), traffic, mineral dust, biomass burning, sea salts (fresh and aged), primary biogenic, and MSA-rich.

A redistribution of the factor impacts between mass and OP contributions was observed, underlining the importance of taking
540   into account the redox activity of PM when considering their potential health effects. Based on PM mass, the major contributors are nitrate- and sulphate-rich factors, both factors being associated with secondary inorganics formed during long range transport (LRT). On the other hand, based on OP activity, the main contributors are mostly anthropogenic-derived sources such as traffic, mineral dust, and biomass burning factors.

As the OPE site is located far from direct anthropogenic emissions, the influence of LRT processes was noted in some sources.
545   Sources such as sulphate- and nitrate-rich, MSA-rich, and aged sea salt factors have shown potential mixing with other anthropogenic sources, most probably due to this transit time. These potential mixing and aging processes were reflected in the chemical mass profile of each factor as well as in their OP contributions.

Thanks to the long-term dataset in the OPE site, it was observed that the traffic factor contribution to total PM_{10} has decreased over the years for this site that may well represent the French national background PM. This effect may be attributed to
550   regulations restricting vehicular emissions in bigger cities and/or other regional-scale influences.

Acknowledgements

The authors wish to thank all the many people (who couldn't be listed exhaustively here) from the different laboratories (OPE, IGE, Air O Sol analytical platform, LCME) and from the regional air quality monitoring network Atmos Grand Est, who actively contributed over the years in filter sampling and/or analysis. The data used for the comparison in Figure 8 is obtained from many different programs, including the CARA program coordinated by O Favez (Favez et al., 2021).

Code availability

The software code is available upon request.

Data availability

The chemical, PMF, and OP datasets are available upon request.

Author contributions

SC manages the overall observatory at OPE, including the supervision of the PM sampling. JLJ designed the project, in collaboration with SC. LB, SW, and AM did the curation of the data base. LB performed the data analysis and wrote the paper. GU manage the OP analytical procedures at IGE. VJ designed part of the analytical method on the Air O Sol plateau. MC is the representation of Atmo GE who helped maintaining the sampling equipment. All authors read and commented the manuscript.

Competing interests

The authors declare that they have no conflict of interest.

References

Aas, W., Tsyro, S., Bieber, E., Bergström, R., Ceburnis, D., Ellermann, T., Fagerli, H., Frölich, M., Gehrig, R., Makkonen, U., Nemitz, E., Otjes, R., Perez, N., Perrino, C., Prévôt, A. S. H., Putaud, J.-P., Simpson, D., Spindler, G., Vana, M., and Yttri, K. E.: Lessons learnt from the first EMEP intensive measurement periods, Atmos. Chem. Phys., 12, 8073–8094, https://doi.org/10.5194/acp-12-8073-2012, 2012.

Alastuey, A., Querol, X., Aas, W., Lucarelli, F., Pérez, N., Moreno, T., Cavalli, F., Areskoug, H., Balan, V., Catrambone, M., Ceburnis, D., Cerro, J. C., Conil, S., Gevorgyan, L., Hueglin, C., Imre, K., Jaffrezo, J.-L., Leeson, S. R., Mihalopoulos, N., Mitosinkova, M., O'Dowd, C. D., Pey, J., Putaud, J.-P., Riffault, V., Ripoll, A., Sciare, J., Sellegri, K., Spindler, G., and Yttri, K. E.: Geochemistry of PM10 over Europe during the EMEP intensive measurement periods in summer 2012 and winter 2013, Atmos. Chem. Phys., 16, 6107–6129, https://doi.org/10.5194/acp-16-6107-2016, 2016.

Alleman, L. Y., Lamaison, L., Perdrix, E., Robache, A., and Galloo, J.-C.: PM10 metal concentrations and source identification using positive matrix factorization and wind sectoring in a French industrial zone, 96, 612–625, https://doi.org/10.1016/j.atmosres.2010.02.008, 2010.

580

Amato, F., Alastuey, A., de la Rosa, J., Gonzalez Castanedo, Y., Sánchez de la Campa, A. M., Pandolfi, M., Lozano, A., Contreras González, J., and Querol, X.: Trends of road dust emissions contributions on ambient air particulate levels at rural, urban and industrial sites in southern Spain, Atmos. Chem. Phys., 14, 3533–3544, https://doi.org/10.5194/acp-14-3533-2014, 2014.

585 Anenberg, S. C., Horowitz, L. W., Tong, D. Q., and West, J. J.: An Estimate of the Global Burden of Anthropogenic Ozone and Fine Particulate Matter on Premature Human Mortality Using Atmospheric Modeling, Environmental Health Perspectives, 118, 1189–1195, https://doi.org/10.1289/ehp.0901220, 2010.

Barrie, L. A. and Hoff, R. M.: Five years of air chemistry observations in the Canadian Arctic, Atmospheric Environment (1967), 19, 1995–2010, https://doi.org/10.1016/0004-6981(85)90108-8, 1985.

590 Bates, J. T., Fang, T., Verma, V., Zeng, L., Weber, R. J., Tolbert, P. E., Abrams, J. Y., Sarnat, S. E., Klein, M., Mulholland, J. A., and Russell, A. G.: Review of Acellular Assays of Ambient Particulate Matter Oxidative Potential: Methods and Relationships with Composition, Sources, and Health Effects, Environ. Sci. Technol., 53, 4003–4019, https://doi.org/10.1021/acs.est.8b03430, 2019.

Belis, C. A.: European guide on air pollution source apportionment with receptor models: revised version 2019., Publications 595 Office, LU, 2019.

Belis, C. A., Pernigotti, D., Karagulian, F., Pirovano, G., Larsen, B. R., Gerboles, M., and Hopke, P. K.: A new methodology to assess the performance and uncertainty of source apportionment models in intercomparison exercises, Atmospheric Environment, 119, 35–44, https://doi.org/10.1016/j.atmosenv.2015.08.002, 2015.

Bernard, Y., Miller, J., Wappelhorst, S., and Braun, C.: Impacts of the Paris Low-Emission Zone and Implications for Other 600 Cities, TRUE - The Real Urban Emissions Initiative, United Kingdom, 2020.

Bessagnet, B., Menut, L., Lapere, R., Couvidat, F., Jaffrezo, J.-L., Mailler, S., Favez, O., Pennel, R., and Siour, G.: High Resolution Chemistry Transport Modeling with the On-Line CHIMERE-WRF Model over the French Alps—Analysis of a Feedback of Surface Particulate Matter Concentrations on Mountain Meteorology, Atmosphere, 11, 565, https://doi.org/10.3390/atmos11060565, 2020.

605 Bilal, M., Nichol, J. E., Nazeer, M., Shi, Y., Wang, L., Kumar, K. R., Ho, H. C., Mazhar, U., Bleiweiss, M. P., Qiu, Z., Khedher, K. M., and Lolli, S.: Characteristics of Fine Particulate Matter (PM2.5) over Urban, Suburban, and Rural Areas of Hong Kong, Atmosphere, 10, 496, https://doi.org/10.3390/atmos10090496, 2019.

Birch, M. E. and Cary, R. A.: Elemental Carbon-Based Method for Monitoring Occupational Exposures to Particulate Diesel Exhaust, Aerosol Science and Technology, 25, 221–241, https://doi.org/10.1080/02786829608965393, 1996.

610 Borlaza, L. J. S., Weber, S., Uzu, G., Jacob, V., Cañete, T., Micallef, S., Trébuchon, C., Slama, R., Favez, O., and Jaffrezo, J.-L.: Disparities in particulate matter (PM₁₀) origins and oxidative potential at a city scale (Grenoble, France) – Part 1: Source apportionment at three neighbouring sites, Atmos. Chem. Phys., 21, 5415–5437, https://doi.org/10.5194/acp-21-5415-2021, 2021.

Borlaza, L. J. S., Weber, S., Jaffrezo, J.-L., Houdier, S., Slama, R., Rieux, C., Albinet, A., Micallef, S., Trébluchon, C., and 615 Uzu, G.: Disparities in particulate matter (PM₁₀) origins and oxidative potential at a city scale

(Grenoble, France) – Part 2: Sources of PM$_{10}$ oxidative potential using multiple linear regression analysis and the predictive applicability of multilayer perceptron neural network analysis, Atmos. Chem. Phys., 21, 9719–9739, https://doi.org/10.5194/acp-21-9719-2021, 2021.

620 Bozzetti, C., El Haddad, I., Salameh, D., Daellenbach, K. R., Fermo, P., Gonzalez, R., Minguillón, M. C., Iinuma, Y., Poulain, L., Elser, M., Müller, E., Slowik, J. G., Jaffrezo, J.-L., Baltensperger, U., Marchand, N., and Prévôt, A. S. H.: Organic aerosol source apportionment by offline-AMS over a full year in Marseille, Atmos. Chem. Phys., 17, 8247–8268, https://doi.org/10.5194/acp-17-8247-2017, 2017.

Brighty, A., Jacob, V., Uzu, G., Borlaza, L. J. S., Conil, S., Hueglin, C., Grange, S., Favez, O., Trebuchon, C., and Jaffrezo, J.-L.: Cellulose in atmospheric particulate matter, 2021.

625 Calas, A., Uzu, G., Martins, J. M. F., Voisin, D., Spadini, L., Lacroix, T., and Jaffrezo, J.-L.: The importance of simulated lung fluid (SLF) extractions for a more relevant evaluation of the oxidative potential of particulate matter, 7, 11617, https://doi.org/10.1038/s41598-017-11979-3, 2017.

Calas, A., Uzu, G., Kelly, F. J., Houdier, S., Martins, J. M. F., Thomas, F., Molton, F., Charron, A., Dunster, C., Oliete, A., Jacob, V., Besombes, J.-L., Chevrier, F., and Jaffrezo, J.-L.: Comparison between five acellular oxidative potential 630 measurement assays performed with detailed chemistry on PM$_{10}$ samples from the city of Chamonix (France), Atmos. Chem. Phys., 18, 7863–7875, https://doi.org/10.5194/acp-18-7863-2018, 2018.

Calas, A., Uzu, G., Besombes, J.-L., Martins, J. M. F., Redaelli, M., Weber, S., Charron, A., Albinet, A., Chevrier, F., Brulfert, G., Mesbah, B., Favez, O., and Jaffrezo, J.-L.: Seasonal Variations and Chemical Predictors of Oxidative Potential (OP) of Particulate Matter (PM), for Seven Urban French Sites, Atmosphere, 10, 698, https://doi.org/10.3390/atmos10110698, 2019.

635 Canonaco, F., Tobler, A., Chen, G., Sosedova, Y., Slowik, J. G., Bozzetti, C., Daellenbach, K. R., El Haddad, I., Crippa, M., Huang, R.-J., Furger, M., Baltensperger, U., and Prévôt, A. S. H.: A new method for long-term source apportionment with time-dependent factor profiles and uncertainty assessment using SoFi Pro: application to 1 year of organic aerosol data, Atmos. Meas. Tech., 14, 923–943, https://doi.org/10.5194/amt-14-923-2021, 2021.

Cassee, F. R., Héroux, M.-E., Gerlofs-Nijland, M. E., and Kelly, F. J.: Particulate matter beyond mass: recent health evidence 640 on the role of fractions, chemical constituents and sources of emission, Inhalation Toxicology, 25, 802–812, https://doi.org/10.3109/08958378.2013.850127, 2013.

Cesari, D., Merico, E., Grasso, F. M., Decesari, S., Belosi, F., Manarini, F., De Nuntiis, P., Rinaldi, M., Volpi, F., Gambaro, A., Morabito, E., and Contini, D.: Source Apportionment of PM2.5 and of its Oxidative Potential in an Industrial Suburban Site in South Italy, Atmosphere, 10, 758, https://doi.org/10.3390/atmos10120758, 2019.

645 Charrier, J. G. and Anastasio, C.: On dithiothreitol (DTT) as a measure of oxidative potential for ambient particles: evidence for the importance of soluble transition metals, Atmos. Chem. Phys., 12, 9321–9333, https://doi.org/10.5194/acp-12-9321-2012, 2012.

Charron, A., Polo-Rehn, L., Besombes, J.-L., Golly, B., Buisson, C., Chanut, H., Marchand, N., Guillaud, G., and Jaffrezo, J.-L.: Identification and quantification of particulate tracers of exhaust and non-exhaust vehicle emissions, Atmos. Chem. Phys., 650 19, 5187–5207, https://doi.org/10.5194/acp-19-5187-2019, 2019.

Chen, Q., Sherwen, T., Evans, M., and Alexander, B.: DMS oxidation and sulfur aerosol formation in the marine troposphere: a focus on reactive halogen and multiphase chemistry, Atmos. Chem. Phys., 18, 13617–13637, https://doi.org/10.5194/acp-18-13617-2018, 2018.

Cho, A. K., Sioutas, C., Miguel, A. H., Kumagai, Y., Schmitz, D. A., Singh, M., Eiguren-Fernandez, A., and Froines, J. R.:
655 Redox activity of airborne particulate matter at different sites in the Los Angeles Basin, Environmental Research, 99, 40–47,
https://doi.org/10.1016/j.envres.2005.01.003, 2005.

Cleveland, R., Cleveland, W., McRae, J., and Terpenning, I.: STL: A seasonal-trend decomposition procedure based on
LOESS, 6, 3–73, 1990.

Conte, E., Canepari, S., Frasca, D., and Simonetti, G.: Oxidative Potential of Selected PM Components, Proceedings, 1, 108,
660 https://doi.org/10.3390/ecas2017-04131, 2017.

Crobeddu, B., Aragao-Santiago, L., Bui, L.-C., Boland, S., and Baeza Squiban, A.: Oxidative potential of particulate matter
2.5 as predictive indicator of cellular stress, Environmental Pollution, 230, 125–133,
https://doi.org/10.1016/j.envpol.2017.06.051, 2017.

Cusack, M., Alastuey, A., Pérez, N., Pey, J., and Querol, X.: Trends of particulate matter (PM$_{2.5}$)
665 and chemical composition at a regional background site in the Western Mediterranean over the last nine years (2002–2010),
Atmos. Chem. Phys., 12, 8341–8357, https://doi.org/10.5194/acp-12-8341-2012, 2012.

Daellenbach, K. R., Uzu, G., Jiang, J., Cassagnes, L.-E., Leni, Z., Vlachou, A., Stefenelli, G., Canonaco, F., Weber, S., Segers,
A., Kuenen, J. J. P., Schaap, M., Favez, O., Albinet, A., Aksoyoglu, S., Dommen, J., Baltensperger, U., Geiser, M., El Haddad,
I., Jaffrezo, J.-L., and Prévôt, A. S. H.: Sources of particulate-matter air pollution and its oxidative potential in Europe, Nature,
670 587, 414–419, https://doi.org/10.1038/s41586-020-2902-8, 2020.

Dou, J., Lin, P., Kuang, B.-Y., and Yu, J. Z.: Reactive Oxygen Species Production Mediated by Humic-like Substances in
Atmospheric Aerosols: Enhancement Effects by Pyridine, Imidazole, and Their Derivatives, Environ. Sci. Technol., 49, 6457–
6465, https://doi.org/10.1021/es5059378, 2015.

Fang, T., Guo, H., Zeng, L., Verma, V., Nenes, A., and Weber, R. J.: Highly Acidic Ambient Particles, Soluble Metals, and
675 Oxidative Potential: A Link between Sulfate and Aerosol Toxicity, Environ. Sci. Technol., 51, 2611–2620,
https://doi.org/10.1021/acs.est.6b06151, 2017.

Favez, O., El Haddad, I., Piot, C., Boréave, A., Abidi, E., Marchand, N., Jaffrezo, J.-L., Besombes, J.-L., Personnaz, M.-B.,
Sciare, J., Wortham, H., George, C., and D'Anna, B.: Inter-comparison of source apportionment models for the estimation of
wood burning aerosols during wintertime in an Alpine city (Grenoble, France), Atmos. Chem. Phys., 10, 5295–5314,
680 https://doi.org/10.5194/acp-10-5295-2010, 2010.

Favez, O., Weber, S., Petit, J.-E., Alleman, L. Y., Albinet, A., Riffault, V., Chazeau, B., Amodeo, T., Salameh, D., Zhang, Y.,
Srivastava, D., Samaké, A., Aujay-Plouzeau, R., Papin, A., Bonnaire, N., Boullanger, C., Chatain, M., Chevrier, F., Detournay,
A., Dominik-Sègue, M., Falhun, R., Garbin, C., Ghersi, V., Grignion, G., Levigoureux, G., Pontet, S., Rangognio, J., Zhang,
S., Besombes, J.-L., Conil, S., Uzu, G., Savarino, J., Marchand, N., Gros, V., Marchand, C., Jaffrezo, J.-L., and Leoz-
685 Garziandia, E.: Overview of the French Operational Network for In Situ Observation of PM Chemical Composition and
Sources in Urban Environments (CARA Program), Atmosphere, 12, 207, https://doi.org/10.3390/atmos12020207, 2021.

Gama, C., Monteiro, A., Pio, C., Miranda, A. I., Baldasano, J. M., and Tchepel, O.: Temporal patterns and trends of particulate
matter over Portugal: a long-term analysis of background concentrations, Air Qual Atmos Health, 11, 397–407,
https://doi.org/10.1007/s11869-018-0546-8, 2018.

690 Gao, D., Ripley, S., Weichenthal, S., and Godri Pollitt, K. J.: Ambient particulate matter oxidative potential: Chemical
determinants, associated health effects, and strategies for risk management, Free Radical Biology and Medicine, 151, 7–25,
https://doi.org/10.1016/j.freeradbiomed.2020.04.028, 2020a.

Gao, D., Mulholland, J. A., Russell, A. G., and Weber, R. J.: Characterization of water-insoluble oxidative potential of PM2.5 using the dithiothreitol assay, Atmospheric Environment, 224, 117327, https://doi.org/10.1016/j.atmosenv.2020.117327, 695 2020b.

Gašparac, G., Jeričević, A., Kumar, P., and Branko, G.: Regional-scale modelling for the assessment of atmospheric particulate matter concentrations at rural background locations in Europe, Aerosols/Atmospheric Modelling/Troposphere/Physics (physical properties and processes), https://doi.org/10.5194/acp-2019-389, 2019.

Gianini, M. F. D., Fischer, A., Gehrig, R., Ulrich, A., Wichser, A., Piot, C., Besombes, J.-L., and Hueglin, C.: Comparative 700 source apportionment of PM10 in Switzerland for 2008/2009 and 1998/1999 by Positive Matrix Factorisation, Atmospheric Environment, 54, 149–158, https://doi.org/10.1016/j.atmosenv.2012.02.036, 2012.

Golly, B., Waked, A., Weber, S., Samake, A., Jacob, V., Conil, S., Rangognio, J., Chrétien, E., Vagnot, M.-P., Robic, P.-Y., Besombes, J.-L., and Jaffrezo, J.-L.: Organic markers and OC source apportionment for seasonal variations of PM2.5 at 5 rural sites in France, Atmospheric Environment, 198, 142–157, https://doi.org/10.1016/j.atmosenv.2018.10.027, 2019.

705 Guascito, M. R., Pietrogrande, M. C., Decesari, S., and Contini, D.: Oxidative Potential of Atmospheric Aerosols, Atmosphere, 12, 531, https://doi.org/10.3390/atmos12050531, 2021.

Hand, J. L., Schichtel, B. A., Pitchford, M., Malm, W. C., and Frank, N. H.: Seasonal composition of remote and urban fine particulate matter in the United States, 117, https://doi.org/10.1029/2011JD017122, 2012.

Handler, M., Puls, C., Zbiral, J., Marr, I., Puxbaum, H., and Limbeck, A.: Size and composition of particulate emissions from 710 motor vehicles in the Kaisermühlen-Tunnel, Vienna, Atmospheric Environment, 42, 2173–2186, https://doi.org/10.1016/j.atmosenv.2007.11.054, 2008.

Henderson, P. and Henderson, G.: The Cambridge handbook of earth science data, Choice Reviews Online, 47, 47-2354-47–2354, https://doi.org/10.5860/CHOICE.47-2354, 2010.

Herich, H., Gianini, M. F. D., Piot, C., Močnik, G., Jaffrezo, J.-L., Besombes, J.-L., Prévôt, A. S. H., and Hueglin, C.: Overview 715 of the impact of wood burning emissions on carbonaceous aerosols and PM in large parts of the Alpine region, Atmospheric Environment, 89, 64–75, https://doi.org/10.1016/j.atmosenv.2014.02.008, 2014.

Jaffrezo, J.-L., Davidson, C. I., Kuhns, H. D., Bergin, M. H., Hillamo, R., Maenhaut, W., Kahl, J. W., and Harris, J. M.: Biomass burning signatures in the atmosphere of central Greenland, J. Geophys. Res., 103, 31067–31078, https://doi.org/10.1029/98JD02241, 1998.

720 Jardine, K., Yañez-Serrano, A. M., Williams, J., Kunert, N., Jardine, A., Taylor, T., Abrell, L., Artaxo, P., Guenther, A., Hewitt, C. N., House, E., Florentino, A. P., Manzi, A., Higuchi, N., Kesselmeier, J., Behrendt, T., Veres, P. R., Derstroff, B., Fuentes, J. D., Martin, S. T., and Andreae, M. O.: Dimethyl sulfide in the Amazon rain forest: DMS in the Amazon, Global Biogeochem. Cycles, 29, 19–32, https://doi.org/10.1002/2014GB004969, 2015.

Jiang, Ahmed, Canchola, Chen, and Lin: Use of Dithiothreitol Assay to Evaluate the Oxidative Potential of Atmospheric 725 Aerosols, Atmosphere, 10, 571, https://doi.org/10.3390/atmos10100571, 2019.

Johnson, D., Utembe, S. R., Jenkin, M. E., Derwent, R. G., Hayman, G. D., Alfarra, M. R., Coe, H., and McFiggans, G.: Simulating regional scale secondary organic aerosol formation during the TORCH 2003 campaign in the southern UK, Atmos. Chem. Phys., 6, 403–418, https://doi.org/10.5194/acp-6-403-2006, 2006.

Kelly, F. J. and Mudway, I. S.: Protein oxidation at the air-lung interface, Amino Acids, 25, 375–396,
730   https://doi.org/10.1007/s00726-003-0024-x, 2003.

Konovalov, I. B., Beekmann, M., Meleux, F., Dutot, A., and Foret, G.: Combining deterministic and statistical approaches for
PM10 forecasting in Europe, Atmospheric Environment, 43, 6425–6434, https://doi.org/10.1016/j.atmosenv.2009.06.039,
2009.

Kulshrestha, M. J., Singh, R., and Ojha, V. N.: Trends and source attribution of PAHs in fine particulate matter at an urban
735   and a rural site in Indo-Gangetic plain, Urban Climate, 29, 100485, https://doi.org/10.1016/j.uclim.2019.100485, 2019.

Lai, A. M., Carter, E., Shan, M., Ni, K., Clark, S., Ezzati, M., Wiedinmyer, C., Yang, X., Baumgartner, J., and Schauer, J. J.:
Chemical composition and source apportionment of ambient, household, and personal exposures to PM2.5 in communities
using   biomass   stoves   in   rural   China,   Science   of   The   Total   Environment,   646,   309–319,
https://doi.org/10.1016/j.scitotenv.2018.07.322, 2019.

740   Li, J., Chen, B., de la Campa, A. M. S., Alastuey, A., Querol, X., and de la Rosa, J. D.: 2005–2014 trends of PM10 source
contributions   in   an   industrialized   area   of   southern   Spain,   Environmental   Pollution,   236,   570–579,
https://doi.org/10.1016/j.envpol.2018.01.101, 2018.

Li, S.-M., Barrie, L. A., Talbot, R. W., Harriss, R. C., Davidson, C. I., and Jaffrezo, J.-L.: Seasonal and geographic variations
of methanesulfonic acid in the arctic troposphere, Atmospheric Environment. Part A. General Topics, 27, 3011–3024,
745   https://doi.org/10.1016/0960-1686(93)90333-T, 1993.

Miyazaki, Y., Fu, P. Q., Kawamura, K., Mizoguchi, Y., and Yamanoi, K.: Seasonal variations of stable carbon isotopic
composition and biogenic tracer compounds of water-soluble organic aerosols in a deciduous forest, Atmos. Chem. Phys., 12,
1367–1376, https://doi.org/10.5194/acp-12-1367-2012, 2012.

Moroni, B., Cappelletti, D., Ferrero, L., Crocchianti, S., Busetto, M., Mazzola, M., Becagli, S., Traversi, R., and Udisti, R.:
750   Local vs. long-range sources of aerosol particles upon Ny-Ålesund (Svalbard Islands): mineral chemistry and geochemical
records, Rend. Fis. Acc. Lincei, 27, 115–127, https://doi.org/10.1007/s12210-016-0533-7, 2016.

Mues, A., Manders, A., Schaap, M., van Ulft, L. H., van Meijgaard, E., and Builtjes, P.: Differences in particulate matter
concentrations between urban and rural regions under current and changing climate conditions, Atmospheric Environment, 80,
232–247, https://doi.org/10.1016/j.atmosenv.2013.07.049, 2013.

755   Nejedlý, Z., Campbell, J. L., Teesdale, W. J., Dlouhy, J. F., Dann, T. F., Hoff, R. M., Brook, J. R., and Wiebe, H. A.: Inter-
Laboratory Comparison of Air Particulate Monitoring Data, Journal of the Air & Waste Management Association, 48, 386–
397, https://doi.org/10.1080/10473289.1998.10463698, 1998.

Nel, A.: ATMOSPHERE: Enhanced: Air Pollution-Related Illness: Effects of Particles, Science, 308, 804–806,
https://doi.org/10.1126/science.1108752, 2005.

760   Norris, G., Duvall, R., Brown, S., and Bai, S.: Positive Matrix Factorization (PMF) 5.0 Fundamentals and User Guide, 136,
2014.

Oh, S.-H., Song, M., Schauer, J. J., Shon, Z.-H., and Bae, M.-S.: Assessment of long-range oriented source and oxidative
potential on the South-west shoreline, Korea: Molecular marker receptor models during shipborne measurements,
Environmental Pollution, 281, 116979, https://doi.org/10.1016/j.envpol.2021.116979, 2021.

765   Paatero, P. and Tapper, U.: Positive matrix factorization: A non-negative factor model with optimal utilization of error estimates of data values, Environmetrics, 5, 111–126, https://doi.org/10.1002/env.3170050203, 1994.

Pandolfi, M., Alastuey, A., Pérez, N., Reche, C., Castro, I., Shatalov, V., and Querol, X.: Trends analysis of PM source contributions and chemical tracers in NE Spainduring 2004–2014: a multi-exponential approach, Atmos. Chem. Phys., 16, 11787–11805, https://doi.org/10.5194/acp-16-11787-2016, 2016.

770   Pappalardo, G.: ACTRIS Aerosol, Clouds and Trace Gases Research Infrastructure, EPJ Web Conf., 176, 09004, https://doi.org/10.1051/epjconf/201817609004, 2018.

Paraskevopoulou, D., Bougiatioti, A., Stavroulas, I., Fang, T., Lianou, M., Liakakou, E., Gerasopoulos, E., Weber, R., Nenes, A., and Mihalopoulos, N.: Yearlong variability of oxidative potential of particulate matter in an urban Mediterranean environment, Atmospheric Environment, 206, 183–196, https://doi.org/10.1016/j.atmosenv.2019.02.027, 2019.

775   Park, M., Joo, H. S., Lee, K., Jang, M., Kim, S. D., Kim, I., Borlaza, L. J. S., Lim, H., Shin, H., Chung, K. H., Choi, Y.-H., Park, S. G., Bae, M.-S., Lee, J., Song, H., and Park, K.: Differential toxicities of fine particulate matters from various sources, Sci Rep, 8, 17007, https://doi.org/10.1038/s41598-018-35398-0, 2018.

Pernigotti, D. and Belis, C. A.: DeltaSA tool for source apportionment benchmarking, description and sensitivity analysis, Atmospheric Environment, 180, 138–148, https://doi.org/10.1016/j.atmosenv.2018.02.046, 2018.

780   Pietrogrande, Russo, and Zagatti: Review of PM Oxidative Potential Measured with Acellular Assays in Urban and Rural Sites across Italy, Atmosphere, 10, 626, https://doi.org/10.3390/atmos10100626, 2019.

Pio, C., Cerqueira, M., Harrison, R. M., Nunes, T., Mirante, F., Alves, C., Oliveira, C., Sanchez de la Campa, A., Artíñano, B., and Matos, M.: OC/EC ratio observations in Europe: Re-thinking the approach for apportionment between primary and secondary organic carbon, Atmospheric Environment, 45, 6121–6132, https://doi.org/10.1016/j.atmosenv.2011.08.045, 2011.

785   Putaud, J.-P., Raes, F., Van Dingenen, R., Brüggemann, E., Facchini, M.-C., Decesari, S., Fuzzi, S., Gehrig, R., Hüglin, C., Laj, P., Lorbeer, G., Maenhaut, W., Mihalopoulos, N., Müller, K., Querol, X., Rodriguez, S., Schneider, J., Spindler, G., Brink, H. ten, Tørseth, K., and Wiedensohler, A.: A European aerosol phenomenology—2: chemical characteristics of particulate matter at kerbside, urban, rural and background sites in Europe, Atmospheric Environment, 38, 2579–2595, https://doi.org/10.1016/j.atmosenv.2004.01.041, 2004.

790   Rinaldi, M., Gilardoni, S., Paglione, M., Sandrini, S., Fuzzi, S., Massoli, P., Bonasoni, P., Cristofanelli, P., Marinoni, A., Poluzzi, V., and Decesari, S.: Organic aerosol evolution and transport observed at Mt. Cimone (2165 m a.s.l.), Italy, during the PEGASOS campaign, Atmos. Chem. Phys., 15, 11327–11340, https://doi.org/10.5194/acp-15-11327-2015, 2015.

Rodríguez González, S., Querol Carceller, X., Universitat Politècnica de Catalunya, and Departament d'Enginyeria Minera i Recursos Naturals: Sources and processes affecting levels and composition of atmospheric particulate matter in the Western
795   Mediterranean, Universitat Politècnica de Catalunya, Barcelona, 2003.

Salvador, P., Artíñano, B., Viana, M., Alastuey, A., and Querol, X.: Evaluation of the changes in the Madrid metropolitan area influencing air quality: Analysis of 1999–2008 temporal trend of particulate matter, Atmospheric Environment, 57, 175–185, https://doi.org/10.1016/j.atmosenv.2012.04.026, 2012.

Samaké, A., Jaffrezo, J.-L., Favez, O., Weber, S., Jacob, V., Albinet, A., Riffault, V., Perdrix, E., Waked, A., Golly, B.,
800   Salameh, D., Chevrier, F., Oliveira, D. M., Bonnaire, N., Besombes, J.-L., Martins, J. M. F., Conil, S., Guillaud, G., Mesbah, B., Rocq, B., Robic, P.-Y., Hulin, A., Le Meur, S., Descheemaecker, M., Chretien, E., Marchand, N., and Uzu, G.: Polyols

and glucose particulate species as tracers of primary biogenic organic aerosols at 28 French sites, Atmos. Chem. Phys., 19, 3357–3374, https://doi.org/10.5194/acp-19-3357-2019, 2019.

805 Scerri, M. M., Kandler, K., and Weinbruch, S.: Disentangling the contribution of Saharan dust and marine aerosol to PM10 levels in the Central Mediterranean, Atmospheric Environment, 147, 395–408, https://doi.org/10.1016/j.atmosenv.2016.10.028, 2016.

Seabold, S. and Perktold, J.: Statsmodels: Econometric and Statistical Modeling with Python, Python in Science Conference, Austin, Texas, 92–96, https://doi.org/10.25080/Majora-92bf1922-011, 2010.

810 Srivastava, D., Tomaz, S., Favez, O., Lanzafame, G. M., Golly, B., Besombes, J.-L., Alleman, L. Y., Jaffrezo, J.-L., Jacob, V., Perraudin, E., Villenave, E., and Albinet, A.: Speciation of organic fraction does matter for source apportionment. Part 1: A one-year campaign in Grenoble (France), Science of The Total Environment, 624, 1598–1611, https://doi.org/10.1016/j.scitotenv.2017.12.135, 2018.

Sun, J., Birmili, W., Hermann, M., Tuch, T., Weinhold, K., Merkel, M., Rasch, F., Müller, T., Schladitz, A., Bastian, S., Löschau, G., Cyrys, J., Gu, J., Flentje, H., Briel, B., Asbach, C., Kaminski, H., Ries, L., Sohmer, R., Gerwig, H., Wirtz, K.,
815 Meinhardt, F., Schwerin, A., Bath, O., Ma, N., and Wiedensohler, A.: Decreasing trends of particle number and black carbon mass concentrations at 16 observational sites in Germany from 2009 to 2018, Atmos. Chem. Phys., 20, 7049–7068, https://doi.org/10.5194/acp-20-7049-2020, 2020.

Tomaz, S., Shahpoury, P., Jaffrezo, J.-L., Lammel, G., Perraudin, E., Villenave, E., and Albinet, A.: One-year study of polycyclic aromatic compounds at an urban site in Grenoble (France): Seasonal variations, gas/particle partitioning and cancer
820 risk estimation, Science of The Total Environment, 565, 1071–1083, https://doi.org/10.1016/j.scitotenv.2016.05.137, 2016.

Tomaz, S., Jaffrezo, J.-L., Favez, O., Perraudin, E., Villenave, E., and Albinet, A.: Sources and atmospheric chemistry of oxy- and nitro-PAHs in the ambient air of Grenoble (France), Atmospheric Environment, 161, 144–154, https://doi.org/10.1016/j.atmosenv.2017.04.042, 2017.

Valko, M., Morris, H., and Cronin, M.: Metals, Toxicity and Oxidative Stress, CMC, 12, 1161–1208,
825 https://doi.org/10.2174/0929867053764635, 2005.

Verma, V., Fang, T., Guo, H., King, L., Bates, J. T., Peltier, R. E., Edgerton, E., Russell, A. G., and Weber, R. J.: Reactive oxygen species associated with water-soluble PM$_{2.5}$ in the southeastern United States: spatiotemporal trends and source apportionment, Atmos. Chem. Phys., 14, 12915–12930, https://doi.org/10.5194/acp-14-12915-2014, 2014.

830 Viana, M., Chi, X., Maenhaut, W., Querol, X., Alastuey, A., Mikuska, P., and Vecera, Z.: Organic and elemental carbon concentrations in carbonaceous aerosols during summer and winter sampling campaigns in Barcelona, Spain, Atmospheric Environment, 40, 2180–2193, https://doi.org/10.1016/j.atmosenv.2005.12.001, 2006.

Visentin, M., Pagnoni, A., Sarti, E., and Pietrogrande, M. C.: Urban PM2.5 oxidative potential: Importance of chemical species and comparison of two spectrophotometric cell-free assays, Environmental Pollution, 219, 72–79,
835 https://doi.org/10.1016/j.envpol.2016.09.047, 2016.

Waked, A., Favez, O., Alleman, L. Y., Piot, C., Petit, J.-E., Delaunay, T., Verlinden, E., Golly, B., Besombes, J.-L., Jaffrezo, J.-L., and Leoz-Garziandia, E.: Source apportionment of PM$_{10}$ in a north-western Europe regional urban background site (Lens, France) using positive matrix factorization and including primary biogenic emissions, 14, 3325–3346, https://doi.org/10.5194/acp-14-3325-2014, 2014.

840 Wang, Y., Wang, M., Li, S., Sun, H., Mu, Z., Zhang, L., Li, Y., and Chen, Q.: Study on the oxidation potential of the water-soluble components of ambient PM2.5 over Xi'an, China: Pollution levels, source apportionment and transport pathways, Environment International, 136, 105515, https://doi.org/10.1016/j.envint.2020.105515, 2020.

Wappelhorst, S. and Muncrief, R.: How can real-world vehicle emissions data help cities to become zero-emission: some evidence from Europe, TRUE – The Real Urban Emissions Initiative, United Kingdom, 2019.

845 Weber, S., Uzu, G., Calas, A., Chevrier, F., Besombes, J.-L., Charron, A., Salameh, D., Ježek, I., Močnik, G., and Jaffrezo, J.-L.: An apportionment method for the oxidative potential of atmospheric particulate matter sources: application to a one-year study in Chamonix, France, Atmos. Chem. Phys., 18, 9617–9629, https://doi.org/10.5194/acp-18-9617-2018, 2018.

Weber, S., Salameh, D., Albinet, A., Alleman, L. Y., Waked, A., Besombes, J.-L., Jacob, V., Guillaud, G., Meshbah, B., Rocq, B., Hulin, A., Dominik-Sègue, M., Chrétien, E., Jaffrezo, J.-L., and Favez, O.: Comparison of PM10 Sources Profiles at 15
850 French Sites Using a Harmonized Constrained Positive Matrix Factorization Approach, Atmosphere, 10, 310, https://doi.org/10.3390/atmos10060310, 2019.

Weber, S., Uzu, G., Favez, O., Borlaza, L. J. S., Calas, A., Salameh, D., Chevrier, F., Allard, J., Besombes, J.-L., Albinet, A., Pontet, S., Mesbah, B., Gille, G., Zhang, S., Pallares, C., Leoz-Garziandia, E., and Jaffrezo, J.-L.: Source apportionment of atmospheric PM₁₀ oxidative potential: synthesis of 15 year-round urban datasets in France, Atmos.
855 Chem. Phys., 21, 11353–11378, https://doi.org/10.5194/acp-21-11353-2021, 2021.

Xiong, Q., Yu, H., Wang, R., Wei, J., and Verma, V.: Rethinking Dithiothreitol-Based Particulate Matter Oxidative Potential: Measuring Dithiothreitol Consumption versus Reactive Oxygen Species Generation, Environ. Sci. Technol., 51, 6507–6514, https://doi.org/10.1021/acs.est.7b01272, 2017.

Yan, C., Nie, W., Äijälä, M., Rissanen, M. P., Canagaratna, M. R., Massoli, P., Junninen, H., Jokinen, T., Sarnela, N., Häme,
860 S., Schobesberger, S., Canonaco, F., Prevot, A. S. H., Petäjä, T., Kulmala, M., Sipilä, M., Worsnop, D. R., and Ehn, M.: Source characterization of Highly Oxidized Multifunctional Compounds in a Boreal Forest Environment using Positive Matrix Factorization, Atmos. Chem. Phys. Discuss., 1–31, https://doi.org/10.5194/acp-2016-367, 2016.

Yang, A., Jedynska, A., Hellack, B., Kooter, I., Hoek, G., Brunekreef, B., Kuhlbusch, T. A. J., Cassee, F. R., and Janssen, N. A. H.: Measurement of the oxidative potential of PM2.5 and its constituents: The effect of extraction solvent and filter type,
865 Atmospheric Environment, 83, 35–42, https://doi.org/10.1016/j.atmosenv.2013.10.049, 2014.

Yazdani, A., Dillner, A. M., and Takahama, S.: Estimating mean molecular weight, carbon number, and OM∕OC with mid-infrared spectroscopy in organic particulate matter samples from a monitoring network, Atmos. Meas. Tech., 14, 4805–4827, https://doi.org/10.5194/amt-14-4805-2021, 2021.

Yu, H., Wei, J., Cheng, Y., Subedi, K., and Verma, V.: Synergistic and Antagonistic Interactions among the Particulate Matter
870 Components in Generating Reactive Oxygen Species Based on the Dithiothreitol Assay, Environ. Sci. Technol., 52, 2261–2270, https://doi.org/10.1021/acs.est.7b04261, 2018.

Zhang, Y., Albinet, A., Petit, J.-E., Jacob, V., Chevrier, F., Gille, G., Pontet, S., Chrétien, E., Dominik-Sègue, M., Levigoureux, G., Močnik, G., Gros, V., Jaffrezo, J.-L., and Favez, O.: Substantial brown carbon emissions from wintertime residential wood burning over France, Science of The Total Environment, 743, 140752, https://doi.org/10.1016/j.scitotenv.2020.140752, 2020.

875